

RESEARCH

Open Access



Identification of a polyphenol O-methyltransferase with broad substrate flexibility in *Streptomyces albidoflavus* J1074

Álvaro Pérez-Valero^{1,2,3}, Patricia Magadán-Corpas^{1,2,3}, Kinga Dulak⁴, Agata Matera⁴, Suhui Ye^{1,2,3}, Ewa Huszcza⁴, Jarosław Popłoński⁴, Claudio J. Villar^{1,2,3} and Felipe Lombó^{1,2,3*}

Abstract

Flavonoids are a large and important group of phytochemicals with a great variety of bioactivities. The addition of methyl groups during biosynthesis of flavonoids and other polyphenols enhances their bioactivities and increases their stability. In a previous study of our research group, we detected a novel flavonoid O-methyltransferase activity in *Streptomyces albidoflavus* J1074, which led to the heterologous biosynthesis of homohesperetin from hesperetin in feeding cultures. In this study, we identify the O-methyltransferase responsible for the generation of this methylated flavonoid through the construction of a knockout mutant of the gene *XNR_0417*, which was selected after a blast analysis using the sequence of a caffeic acid 3'-O-methyltransferase from *Zea mays* against the genome of *S. albidoflavus* J1074. This mutant strain, *S. albidoflavus* Δ XNR_0417, was no longer able to produce homohesperetin after hesperetin feeding. Subsequently, we carried out a genetic complementation of the mutant strain in order to confirm that the enzyme encoded by *XNR_0417* is responsible for the observed O-methyltransferase activity. This new strain, *S. albidoflavus* SP43-XNR_0417, was able to produce not only homohesperetin from hesperetin, but also different mono-, di-, tri- and tetra-methylated derivatives on other flavanones, flavones and stilbenes, revealing a broad substrate flexibility. Additionally, in vitro experiments were conducted using the purified enzyme on the substrates previously tested in vivo, demonstrating doubtless the capability of XNR_0417 to generate various methylated derivatives.

Keywords Flavonoid, O-Methyltransferase, *Streptomyces*, Methylation, Substrate flexibility

Background

Polyphenols are the largest group of phytochemicals known in nature. They have been associated to a variety of health benefits, such as the prevention of cancer, cardiovascular and neurodegenerative diseases [1]. Polyphenols comprise different families, such as flavonoids and stilbenes. Flavonoids are a huge family of nutraceutical compounds widely distributed in plants, including dietary plants [1–5]. On the other hand, stilbenes represent a relatively small group of phytochemicals found in grapes, peanuts, rhubarb, berries, etc. [6, 7].

*Correspondence:

Felipe Lombó

lombofelipe@uniovi.es

¹ Research Group BIONUC (Biotechnology of Nutraceuticals and Bioactive Compounds), Departamento de Biología Funcional, Área de Microbiología, Universidad de Oviedo, Oviedo, Principality of Asturias, Spain

² IUOPA (Instituto Universitario de Oncología del Principado de Asturias), Oviedo, Principality of Asturias, Spain

³ ISPA (Instituto de Investigación Sanitaria del Principado de Asturias), Oviedo, Principality of Asturias, Spain

⁴ Department of Food Chemistry and Biocatalysis, Wrocław University of Environmental and Life Sciences, Norwida 25, 50-375 Wrocław, Poland



© The Author(s) 2024. **Open Access** This article is licensed under a Creative Commons Attribution-NonCommercial-NoDerivatives 4.0 International License, which permits any non-commercial use, sharing, distribution and reproduction in any medium or format, as long as you give appropriate credit to the original author(s) and the source, provide a link to the Creative Commons licence, and indicate if you modified the licensed material. You do not have permission under this licence to share adapted material derived from this article or parts of it. The images or other third party material in this article are included in the article's Creative Commons licence, unless indicated otherwise in a credit line to the material. If material is not included in the article's Creative Commons licence and your intended use is not permitted by statutory regulation or exceeds the permitted use, you will need to obtain permission directly from the copyright holder. To view a copy of this licence, visit <http://creativecommons.org/licenses/by-nc-nd/4.0/>.

Flavonoids share a canonical structure of 15 carbon atoms (C₆–C₃–C₆). The core chemical structure contains two aromatic rings (ring A and B) connected by a heterocyclic tetrahydropyran moiety (ring C) [8, 9] (Fig. 1). Stilbenes show a carbon skeleton with the structure of 1,2-diphenylethylene (C₆–C₂–C₆), consisting of an ethylene moiety connecting two benzene rings [10] (Fig. 1). Flavonoids have been investigated as antimicrobial, antiangiogenic [11, 12], antitumor [11–13], and antioxidant compounds [14], among other bioactivities. Likewise, stilbenes have demonstrated a wide range of biological activities, such as antimicrobial [15], antifungal [16], anti-inflammatory [17] and antitumor [18], among others [19].

Methylated derivatives of flavonoids and stilbenes also display interesting bioactivities [20, 21] and show improved oral bioavailability, better stability and better absorption due to the enhanced lipophilicity conferred by the methyl groups [22, 23]. Both, flavonoid and stilbene methylated derivatives, are less common in their natural plant producers than the unmethylated forms [24, 25], hindering the extraction of large quantities. An alternative to the extraction from their natural producers is the chemical synthesis. However, this requires the chemical blocking and deblocking steps to introduce the methyl moieties in the desired positions of the final substrate [26]. In this context, the biotransformation (using microbial factories) emerges as a promising method to modify flavonoid backbones [27]. Regarding this, it is interesting to search methyltransferases in different organisms for à la carte polyphenols tailoring.

In the databases, a plethora of polyphenol O-methyltransferases (OMTs) have been identified in different plant species. Also, several polyphenol OMTs have also been found in bacteria, especially in the genus *Streptomyces* [28–32]. In recent studies of our research group, we have observed a native flavonoid OMT activity in *Streptomyces albidoflavus* J1074 able to generate eriodictyol

3',4'-dimethyl ether (homohesperetin) from eriodictyol 4'-methyl ether (hesperetin) feeding [33]. Furthermore, we putatively identified a compound as luteolin 3',4'-dimethyl ether during the biosynthesis of luteolin 4'-methyl ether (diosmetin) and luteolin 3'-methyl ether (chrysoeriol) feeding, which was attributed to this *S. albidoflavus* OMT activity [34]. However, the bacterial gene encoding this enzymatic activity remained unknown.

In this study, we have identified the gene encoding the OMT of *S. albidoflavus* J1074 responsible of the abovementioned methylations and have demonstrated its activity in vivo. Moreover, we have tested the substrate flexibility of the encoded enzyme either in vivo and in vitro using different polyphenols, specifically flavanones, flavones, and stilbenes.

Results

Selection of a candidate gene encoding the flavonoid OMT of *S. albidoflavus* J1074

Streptomyces albidoflavus J1074 (accession number: CP004370.1) has numerous methyltransferase genes annotated in its genome, but only seven are annotated as OMTs. According to our previous results, the targeted flavonoid OMT activity in *S. albidoflavus* J1074 seems to have a preference for introducing a methyl group in position 3' of the ring B of hesperetin [33]. With the aim of identifying the responsible enzyme for this flavonoid OMT activity, we performed a BLASTP analysis using the amino acid sequence of a caffeic acid 3'-OMT from *Zea mays* (accession number: NP_001106047.1) against the genome of *S. albidoflavus* J1074. The results showed only one hit, with 35% of identity, 49% positives and 6% gaps. This hit corresponded to *XNR_0417*, a gene encoding one of the seven annotated OMTs in this species.

Additionally, we found that the gene *XNR_0417* overlaps with the gene *XNR_0418* on the chromosome of *Streptomyces albidoflavus* J1074. According to genome annotations, *XNR_0418* encodes a

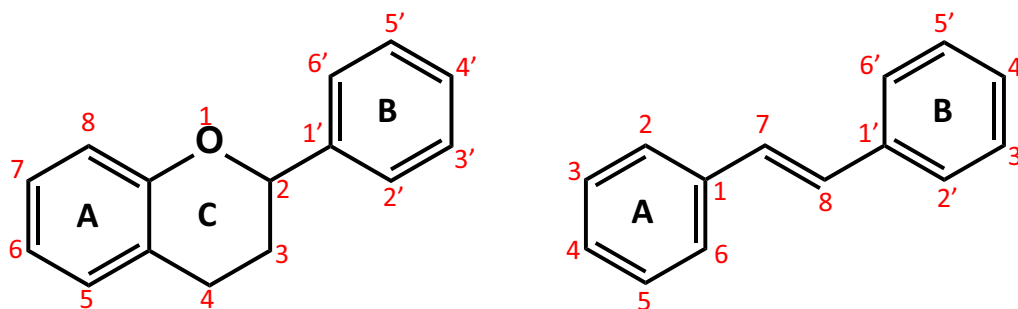


Fig. 1 Basic skeleton of flavonoids (left) and stilbenes (right). Carbon positions are displayed in red color

hypothetical protein. However, BLASTP analysis of the amino acid sequence of XNR_0417 revealed a high number of hits showing similarity with holin proteins, exhibiting identities exceeding 99%. Holins are small membrane proteins specific to bacteriophages and are essential for the degradation of the host cell envelope [35]. This finding indicates that the XNR_0417 OMT may have a viral origin.

With the aim of obtaining more information related to this protein, a phylogenetic analysis was performed using not only flavonoid OMTs from plants and *Streptomyces*, but also OMTs from bacteriophages (Figures S1). After this analysis, we found that this protein is more closely related to flavonoid OMTs from *Streptomyces* than to those OMTs from plant or bacteriophages. Taking into account the overlap of the gene XNR_0417 with the gene XNR_0418, which encodes a holin-type protein, and the results obtained from the phylogenetic analysis, it is possible that the integration of a phage genome harboring these genes occurred in a *Streptomyces* ancestor long ago during evolution.

Effect of deletion of the gene XNR_0417 in *S. albidoflavus* J1074

A knockout mutant strain of XNR_0417 was generated in *S. albidoflavus* J1074 in order to establish a correlation between its encoded enzyme and the specific OMT activity under investigation. This mutant strain, named as *S. albidoflavus* ΔXNR_0417, was generated using the CRISPR-based plasmid pSEVAUO-C41012-XNR_0417 (Figure S2).

Then, both *S. albidoflavus* J1074 and *S. albidoflavus* ΔXNR_0417 strains were cultivated in the presence of hesperetin (see “Material and methods” section) and, 5 days after inoculation, samples were extracted with organic solvents, and the extracts were analyzed by high performance liquid chromatography with diode array detector (HPLC–DAD). The corresponding chromatograms showed a significant accumulation of hesperetin in both extracts. However, only the extract from *S. albidoflavus* J1074 contained the methylated derivative homohesperetin, while this was absent in the extract from *S. albidoflavus* ΔXNR_0417 mutant strain. These results were corroborated using authentic pure standards of hesperetin and homohesperetin (Fig. 2). This experiment allowed to identify the enzyme encoded by XNR_0417 as the responsible one for the studied native OMT activity in this actinomycete.

Phenotypic complementation of the XNR_0417 knockout mutant strain

In order to confirm that the gene XNR_0417 actually encodes the OMT which converts hesperetin to homohesperetin, a phenotypic complementation of the strain *S. albidoflavus* ΔXNR_0417 was carried out. Plasmid pSEVAUO-M21402-XNR_0417, harboring the XNR_0417 gene sequence under the control of the strong constitutive promoter SP43 [36], was integrated into the φBT1 *attB* site of the chromosome of *S. albidoflavus* ΔXNR_0417 mutant strain, giving rise to the strain *S. albidoflavus* SP43-XNR_0417.

This new strain was cultivated in parallel with its parental mutant strain *S. albidoflavus* ΔXNR_0417 in the presence of hesperetin. After 5 days of fermentation, samples were extracted and analyzed by HPLC–DAD. As expected, the production of homohesperetin (compound 5, Fig. 3A) from hesperetin (compound 3) was restored in *S. albidoflavus* SP43-XNR_0417. Moreover, three new compounds (2', 4 and 6) were detected in this extract (Fig. 3A), whose identities remain unknown. Thus, it seems that the XNR_0417 enzyme may have substrate flexibility and that placing the gene XNR_0417 under the control of the strong and constitutive promoter SP43 leads to higher doses of this enzyme, which enables the detection of these new putative methylated derivatives.

In vivo assays to determine the substrate flexibility of XNR_0417 on different flavanones, flavones, and stilbenes

In order to determine the substrate flexibility of the XNR_0417 OMT enzyme on other polyphenols, two additional flavanones, three flavones and three stilbenes were tested in vivo using the strain *S. albidoflavus* SP43-XNR_0417 and the strain *S. albidoflavus* ΔXNR_0417 (as a negative control).

Flavanones

In the case of flavanones, hesperetin (C₁₆H₁₄O₆), eriodictyol (C₁₅H₁₂O₆), homoeriodictyol (C₁₆H₁₄O₆) and homohesperetin (C₁₇H₁₆O₆) were tested. The Fig. 3B–D show the HPLC–DAD chromatograms of the strains *S. albidoflavus* SP43-XNR_0417 and *S. albidoflavus* ΔXNR_0417 after feeding with eriodictyol, homoeriodictyol and homohesperetin, respectively. In the case of the eriodictyol feeding, the compounds 1 (eriodictyol), 2 (homoeriodictyol), 4, 5 (homohesperetin, C₁₇H₁₆O₆) and 6 were detected (Fig. 3B) in the extract of the strain *S. albidoflavus* SP43-XNR_0417. However, only the compound 1 (eriodictyol) was detected in the extract of the control mutant strain.

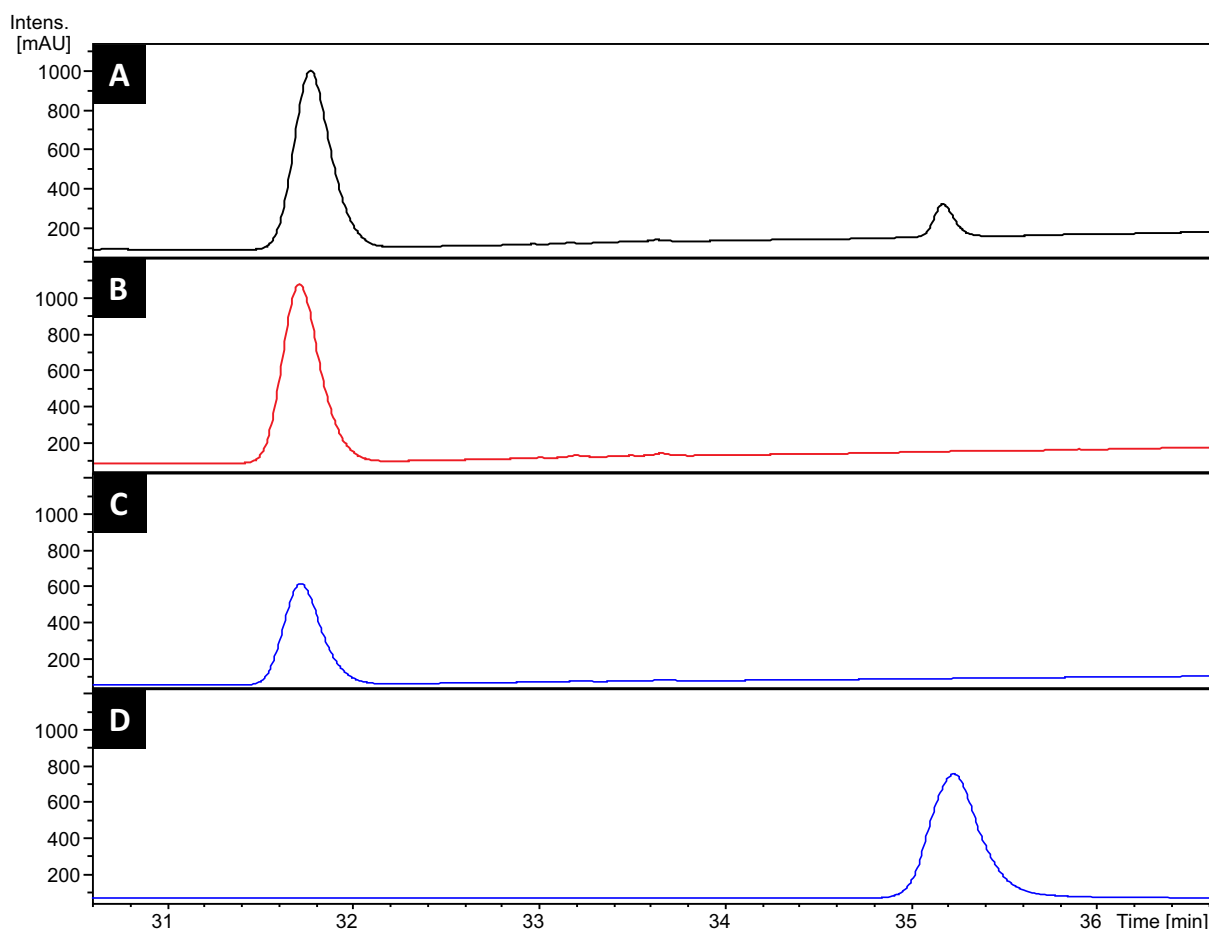


Fig. 2 HPLC–DAD chromatograms of *S. albidoflavus* J1074 + hesperetin (A), *S. albidoflavus* Δ XNR_0417 + hesperetin (B), authentic pure standard of hesperetin (C) and authentic pure standard of homohesperetin (D)

On the other hand, the compounds 2 (homoeriodictyol), 4, 5 (homohesperetin) and 6 were detected after homoeriodictyol feeding (Fig. 3C) in the strain expressing the *XNR_0417* gene, and only the compound 2 (homoeriodictyol) was detected in the control mutant strain.

Regarding homohesperetin feeding (Fig. 3D), compounds 5 (homohesperetin) and 6 were detected in the strain harboring the *XNR_0417* gene.

Eriodictyol (compound 1), homoeriodictyol (compound 2), hesperetin (compound 3) and homohesperetin (compound 5) were identified using commercial pure standards (Fig. 3E). As mentioned above, one of the new detected compounds after hesperetin feeding was compound 2'. This compound had the same retention time that homoeriodictyol (Fig. 3A, E), however, it showed a different absorption spectrum (Figure S3).

To obtain more information on the compounds generated from these flavanones feedings, the samples were analyzed by high performance liquid chromatography

coupled to electrospray ionization high resolution mass spectrometry (HPLC–HRESIMS). In the following paragraphs, the A compounds indicate flavonoids showing m/z ions according to the presence of three methyl groups in the flavonoid skeleton, the B compounds indicate flavonoids showing m/z ions according to the presence of one methyl group in the flavonoid skeleton, the C compounds indicate flavonoids showing m/z ions according to the presence of two methyl groups in the flavonoid skeleton, and the D compounds indicate flavonoids showing m/z ions according to the presence of four methyl groups in the flavonoid skeleton.

In the extract of *S. albidoflavus* SP43-XNR_0417 after the hesperetin ($C_{16}H_{14}O_6$) feeding, the signals A1, A3 and A4 (all with an m/z 329.1030618 $[M-H]^-$, calculated for $C_{18}H_{18}O_6$, involving a total of three methyl groups present in the flavonoid skeleton) were detected. Three more signals; B1, C2, and D, with m/z $[M-H]^-$ of 301.0717617 (calculated for $C_{16}H_{14}O_6$, hesperetin), 315.0874118 (calculated for $C_{17}H_{16}O_6$, homohesperetin) and 343.1187119

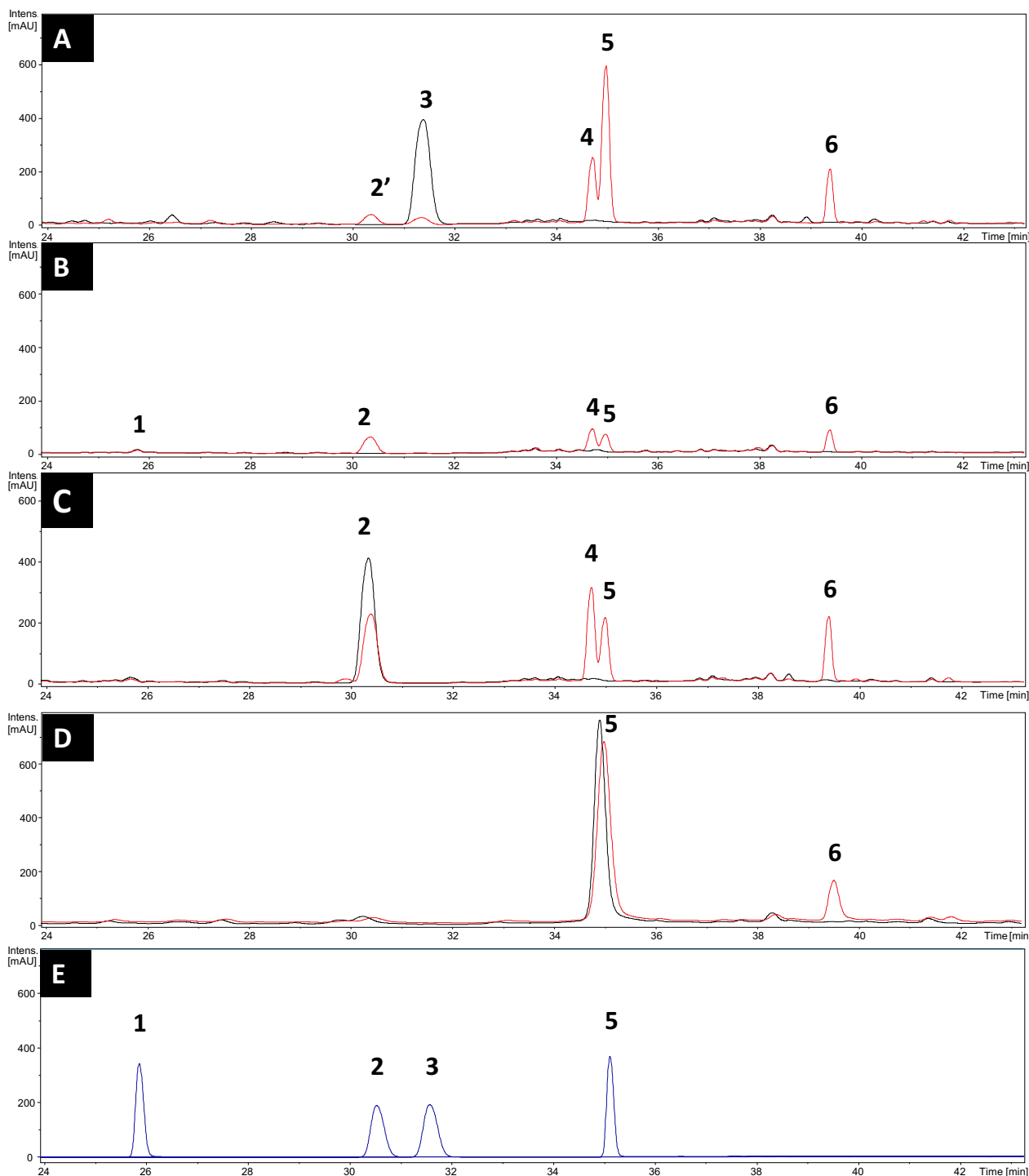


Fig. 3 HPLC–DAD chromatograms of cultures of *S. albidoflavus* ΔXNR_0417 (black) and *S. albidoflavus* SP43-XNR_0417 (red) after addition of **A** hesperetin 0.1 mM; **B** eriodictyol 0.1 mM; **C** homoeriodictyol 0.1 mM; and **D** homohesperetin 0.1 mM. **E** Authentic pure standards of eriodictyol (1), homoeriodictyol (2), hesperetin (3), and homohesperetin (5). Peaks 2' and 6 are unknown compounds

(calculated for $C_{19}H_{20}O_6$, involving a total of four methyl groups present in the flavonoid skeleton), respectively, were also detected (Figs. 4(1) and 5).

In the case of the eriodictyol ($C_{15}H_{12}O_6$) feeding (Fig. 4(2)), the signals A3 and A4 (m/z 329.1030618 $[M-H]^-$, calculated for $C_{18}H_{18}O_6$) were detected (involving the presence of a total of three methyl groups). The

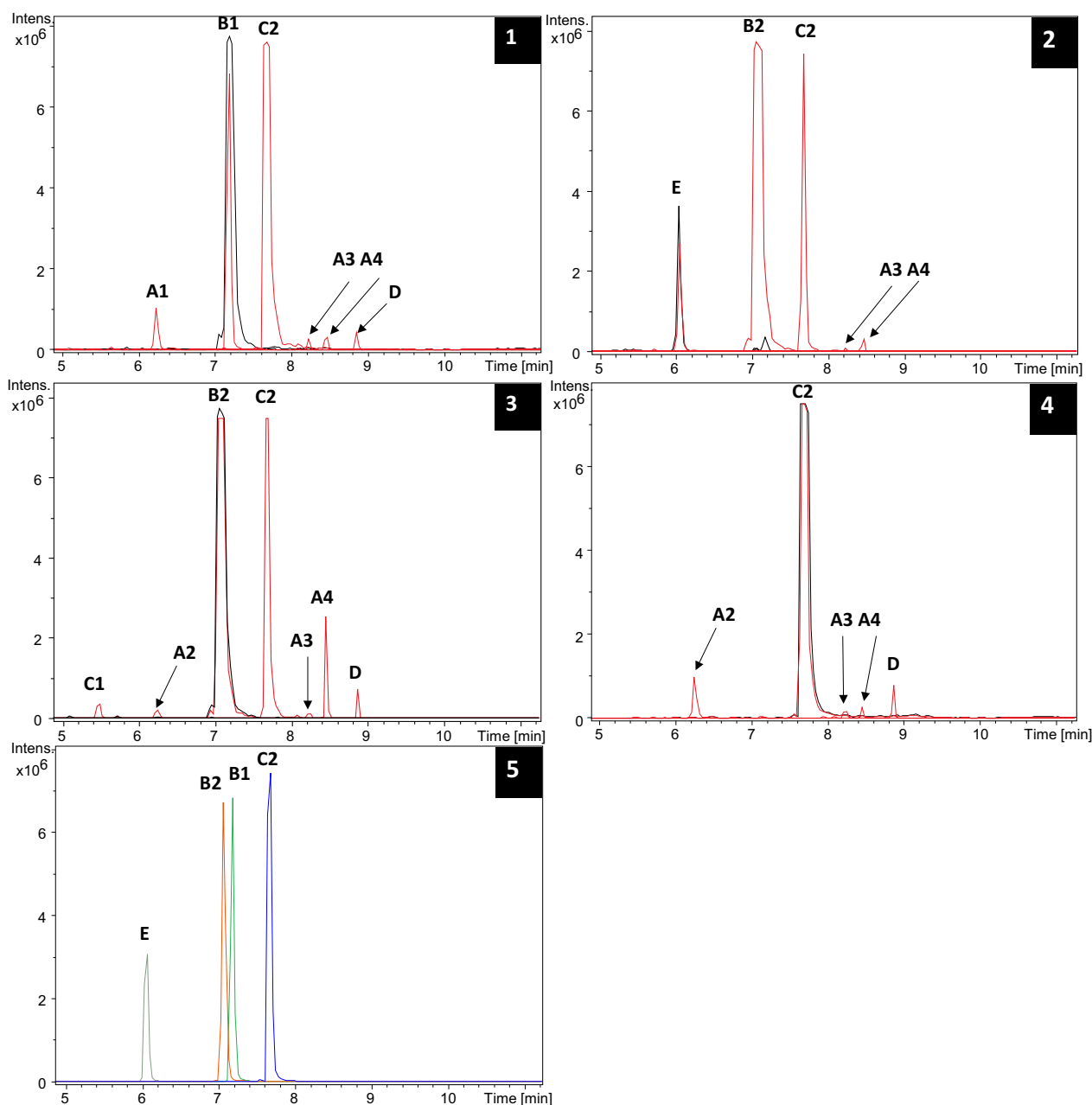


Fig. 4 HPLC-HRESIMS chromatograms of the strains *S. albidoflavus* SP43-XNR_0417 (red) and *S. albidoflavus* ΔXNR_0417 (black) after feeding with flavanones; **1** hesperetin, **2** eriodictyol, **3** homoeriodictyol and **4** homohesperetin. **5** Pure standards of eriodictyol (**E**, gray), homoeriodictyol (**B2**, red), hesperetin (**B1**, green) and homohesperetin (**C2**, blue). Capital letters corresponds to extracted ion chromatograms (EICs) for different m/z $[M-H]^-$: (**A1–A4**): 329.1030618 (calculated for $C_{18}H_{18}O_6$: flavonoid skeletons with a total of three present methyl groups), (**B1, B2**): 301.0717617 (calculated for $C_{16}H_{14}O_6$: flavonoid skeletons with a total of one methyl group), (**C1, C2**): 315.0874118 (calculated for $C_{17}H_{16}O_6$: flavonoid skeletons with a total of two methyl groups), (**D**): 343.1187119 (calculated for $C_{19}H_{20}O_6$: flavonoid skeleton with a total of four methyl groups), and (**E**): 287.0561117 (calculated for $C_{15}H_{12}O_6$: flavonoid skeleton without methyl groups). Capital letters followed by different numbers correspond to different compounds with the same m/z $[M-H]^-$

signals B2 (m/z $[M-H]^-$ of 301.0717617, calculated for $C_{16}H_{14}O_6$, corresponding to homoeriodictyol), C2 (m/z $[M-H]^-$ of 315.0874118, calculated for $C_{17}H_{16}O_6$, corresponding to homohesperetin) and E (m/z $[M-H]^-$ of

287.0561117, calculated for $C_{15}H_{12}O_6$, corresponding to eriodictyol), were detected as well (see also Fig. 5).

On the other hand, after homoeriodictyol ($C_{16}H_{14}O_6$) feeding, the signals A2, A3 and A4 (m/z 329.1030618

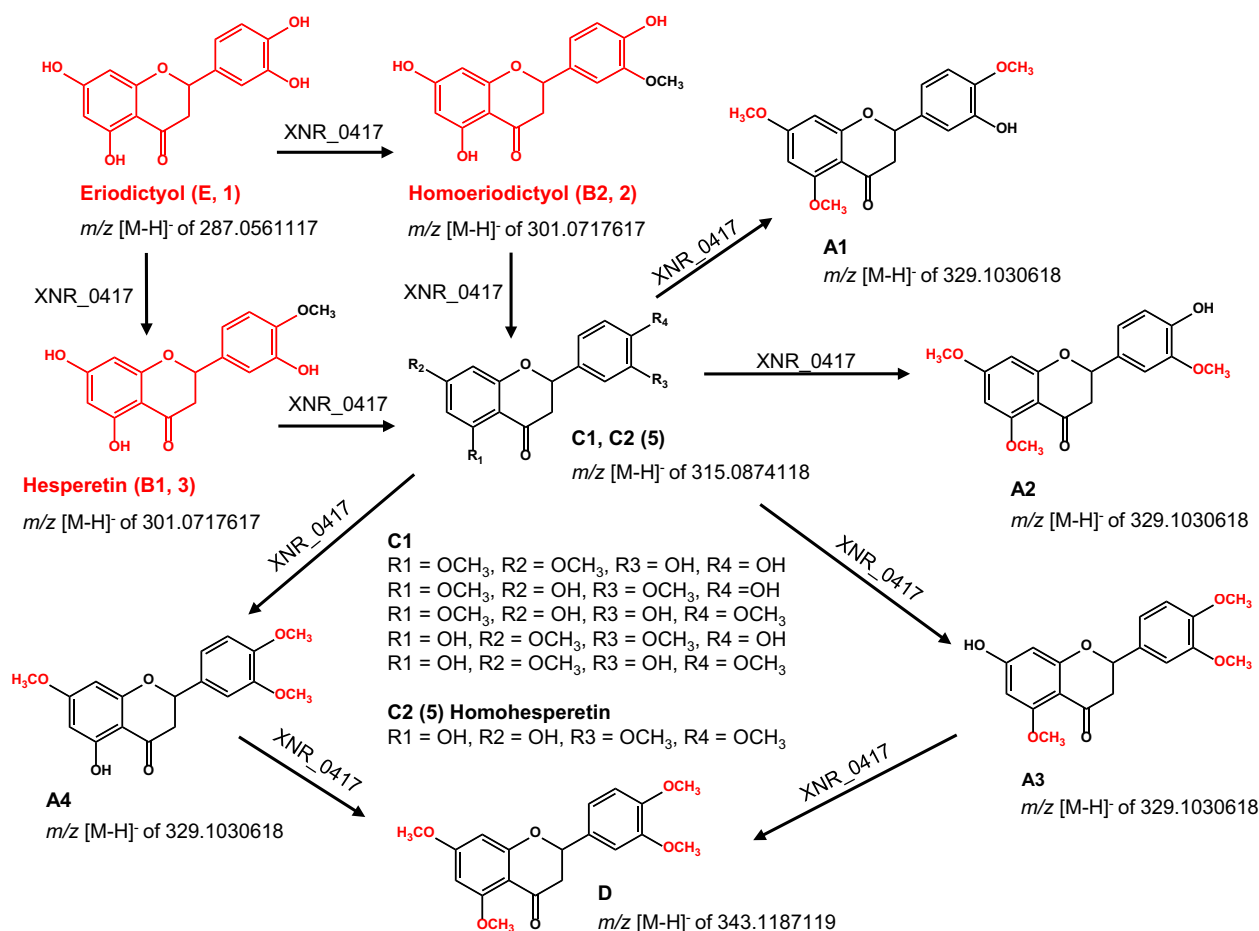


Fig. 5 Proposed compounds generated by the XNR_0417 OMT from the different flavanones tested as substrate. Flavanones used in the feeding experiments are depicted in red. The *O*-methyl groups introduced by XNR_0417 are highlighted in different color within the structures. Compounds are named as the detected signals of m/z [M-H]⁻ (compounds corroborated with authentic pure standards are also named with their assigned number in the HPLC-DAD analysis). Compound C1, containing R in its structure, is unknown and can correspond to one of the possible *O*-methyl groups distribution described next to its structure

[M-H]⁻, calculated for C₁₈H₁₈O₆), C1 and C2 (with m/z [M-H]⁻ of 315.0874118, calculated for C₁₇H₁₆O₆) were detected. The signals B2 (homoeriodictyol) and D (with m/z [M-H]⁻ of 343.1187119, calculated for C₁₉H₂₀O₆) were also detected (Figs. 4(3) and 5).

Finally, after homohesperetin (C₁₇H₁₆O₆) feeding, the signals A2, A3 and A4 (m/z 329.1030618 [M-H]⁻, calculated for C₁₈H₁₈O₆), C2 (with m/z [M-H]⁻ of 315.0874118, calculated for C₁₇H₁₆O₆, corresponding to homohesperetin) and D (with m/z [M-H]⁻ of 343.1187119, calculated for C₁₉H₂₀O₆) were detected (Figs. 4(4) and 5).

The Fig. 4(5) shows the Base Peak Chromatograms (BPCs) of signals E, B1, B2 and C2, corresponding to eriodictyol, homoeriodictyol, hesperetin and homohesperetin pure standards, respectively.

The A type signals have a m/z [M-H]⁻ corresponding to eriodictyol trimethyl ethers (C₁₈H₁₈O₆). Since this

type of signal appears three times after hesperetin feeding (A1, A3 and A4) and homoeriodictyol and homohesperetin feedings (A2, A3 and A4) (Fig. 4(1, 3)), the presence of three different forms of eriodictyol trimethyl ethers in these extracts is a possibility, while two of these forms (A3 and A4) were present in the extract generated after eriodictyol feeding (Fig. 4(2)).

In the case of the hesperetin feeding, the signal B1 was assigned to hesperetin using a pure standard, and it corresponds to peak 3 in Fig. 3A. On the other hand, in extracts from the eriodictyol and homoeriodictyol feedings, the signal B2 (C₁₆H₁₄O₆) was confirmed as homoeriodictyol using its pure standard, and it corresponds to peak 2 in Figs. 3B, C. The signal C (C₁₇H₁₆O₆) appears once in the extracts of the hesperetin, eriodictyol and homohesperetin feedings (C2) and it was confirmed as homohesperetin using a pure standard. However, in

the extract from the homoeriodictyol feeding, the signal C appears twice (C1 and C2). The signal C1, that appears at early retention time, remains unknown. The signal D ($C_{19}H_{20}O_6$) is detected only in the extracts of the hesperetin, homoeriodictyol and homohesperetin feedings, and it shows a m/z 343.1187119 $[M-H]^-$ that corresponds to an eriodictyol tetramethyl ether, which is the eriodictyol molecule with all the hydroxyl moieties substituted by a methyl group. This peak could not be related with none of those observed by HPLC–DAD analysis (Fig. 3) since it only appears after hesperetin, homoeriodictyol and homohesperetin feedings and no differential peaks were detected by HPLC–DAD between these three conditions and the eriodictyol feeding. Finally, the signal E was confirmed as eriodictyol ($C_{15}H_{12}O_6$) using a pure standard, and it corresponds to the compound 1 in Fig. 3. This signal is only detected after eriodictyol feeding, either in *S. albidoflavus* SP43-XNR_0417 and the control strain. All the proposed flavanone *O*-methylated derivatives detected by HPLC–HRESIMS are represented in Fig. 5.

Flavones

The flavones tested as potential substrates of XNR_0417 enzyme were luteolin, diosmetin and chrysoeriol. Figure 6 shows the HPLC–DAD chromatograms of the strains *S. albidoflavus* SP43-XNR_0417 and *S. albidoflavus* Δ XNR_0417 after feeding with luteolin (Fig. 6A), diosmetin (Fig. 6B) and chrysoeriol (Fig. 6C). Luteolin, chrysoeriol and diosmetin were identified as the compounds 7, 8 and 9 respectively, using pure standards (Fig. 6D). In the case of the luteolin feeding, the compounds 7, 8, 10 and 11 were detected in the extract of the strain *S. albidoflavus* SP43-XNR_0417, but only the compound 7 was detected in the extract of *S. albidoflavus* Δ XNR_0417. After the diosmetin feeding, only the compounds 10 and 11 were detected in the strain harboring XNR_0417, while the compound 9 was accumulated in the negative control strain. Finally, the compounds 8, 10 and 11 were detected after the chrysoeriol feeding in the extract of *S. albidoflavus* SP43-XNR_0417, but in the negative control strain only the compound 8 was detected. The identity of the compounds 10 and 11 remains unknown.

These samples were also analyzed by HPLC–HRESIMS (Fig. 7). In the extract of *S. albidoflavus* SP43-XNR_0417 after luteolin feeding, the signals F (m/z 285.0404616 $[M-H]^-$, calculated for $C_{15}H_{10}O_6$), G1 (m/z 299.0561117 $[M-H]^-$, calculated for $C_{16}H_{12}O_6$, indicating the presence of a total of one methyl group), H (m/z 313.0717617 $[M-H]^-$, calculated for $C_{17}H_{14}O_6$, indicating the presence of a total of two methyl groups) and I2 (m/z 327.0874118 $[M-H]^-$, calculated for

$C_{18}H_{16}O_6$, indicating the presence of a total of three methyl groups) were detected (Fig. 7(1)). The signals F and G1 were also detected in the control strain. The signal G1 was identified as chrysoeriol using a pure standard. The presence of the signal G1 in the control strain may correspond to chrysoeriol or any other compound produced by *S. albidoflavus*. However, the presence of chrysoeriol in the control strain would not be surprising since different flavonoid OMTs have been reported in other *Streptomyces* species [29–32, 37].

In the case of the diosmetin feeding (Fig. 7(2)), the signals G2 (m/z 299.0561117 $[M-H]^-$, calculated for $C_{16}H_{12}O_6$, indicating the presence of a total of one methyl group), H (m/z 313.0717617 $[M-H]^-$, calculated for $C_{17}H_{14}O_6$, indicating the presence of a total of two methyl groups), I1 and I2 (m/z 327.0874118 $[M-H]^-$, calculated for $C_{18}H_{16}O_6$, indicating the presence of a total of three methyl groups) were detected in the strain *S. albidoflavus* SP43-XNR_0417. Only the signal G2 was detected in the negative control strain.

After the feeding with chrysoeriol, the signals G1, H, I1 and I2 were detected in the strain harboring XNR_0417. Only the signal G1 was detected in the control strain (Fig. 7(3)). The Fig. 7(4) shows the extracted BPCs of the pure standards luteolin (F), chrysoeriol (G1) and diosmetin (G2).

Chrysoeriol (G1) and diosmetin (G2) have the same molecular mass and thus, the same m/z $[M-H]^-$. On the other hand, the signal H, which appears in the strain *S. albidoflavus* SP43-XNR_0417 after the feeding with the three flavones, has a m/z 313.0717617 $[M-H]^-$ that corresponds to a dimethylated luteolin. In a previous work of our research group, we detected a putative luteolin 3',4'-dimethyl ether during the heterologous biosynthesis of diosmetin and chrysoeriol in a strain of *S. albidoflavus* [34], and it presents the same retention time that peak 10 in Fig. 6C. This indicates that the compound 10 and the signal H may correspond to luteolin 3',4'-dimethyl ether.

Finally, the signals I1 and I2 have the m/z $[M-H]^-$ of luteolin trimethyl ether. I2 is detected in the case of luteolin feeding, and I1 and I2 are detected both in the diosmetin and chrysoeriol feedings. Since the signal I2 is common in all the feedings, it may correspond to the compound 11 in Fig. 6, while the signal I1 cannot be related with any peak in the HPLC–DAD analysis. In the case of flavones, no signals corresponding to tetra-methylated derivatives were detected. All the proposed flavone *O*-methylated derivatives detected by HPLC–DAD and HPLC–HRESIMS are represented in Fig. 8.

Stilbenes

The stilbenes tested as possible substrates for the XNR_0417 enzyme were resveratrol, rhapontin and

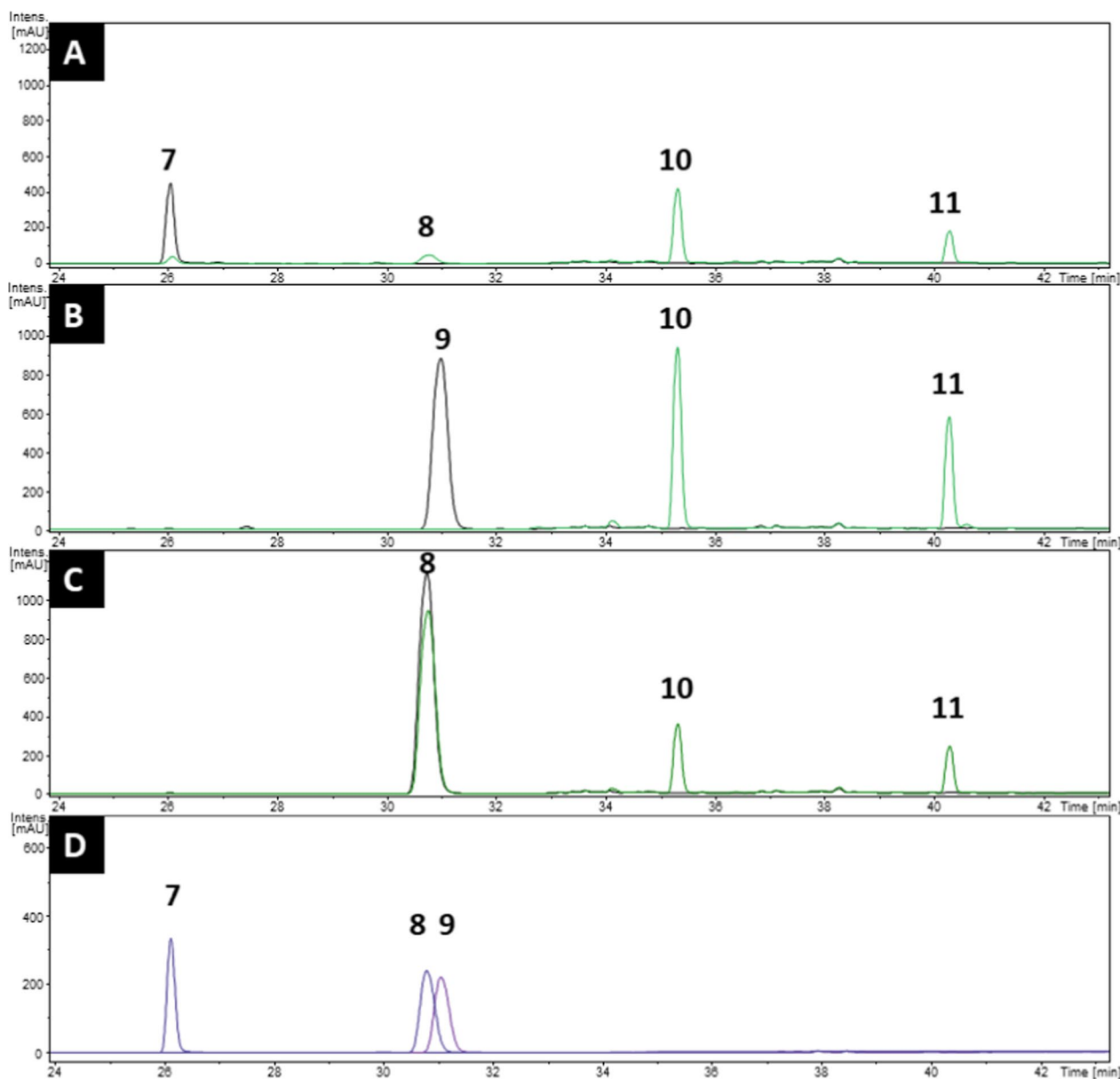


Fig. 6 HPLC–DAD chromatograms of cultures of *S. albidoflavus* Δ XNR_0417 (black) and *S. albidoflavus* SP43-XNR_0417 (green) after addition of **A** luteolin 0.1 mM; **B** diosmetin 0.1 mM; and **C** chrysoeriol 0.1 mM. **D** Authentic pure standards of luteolin (7), chrysoeriol (8), and diosmetin (9). Peaks 10 and 11 are unknown

polydatin, being the last two ones glycosylated stilbenes. Figure 9 shows HPLC–DAD chromatograms of the strains *S. albidoflavus* SP43-XNR_0417 and *S. albidoflavus* Δ XNR_0417 after the feeding with resveratrol (Fig. 9A), rhapontin (Fig. 9B) and polydatin (Fig. 9C). Resveratrol, rhapontin and polydatin were identified as the compounds 14, 13 and 12 respectively using pure standards (Fig. 9D). After the feeding with resveratrol, the compounds 14, 17, 18, 19 and 21 were detected in the

strain harboring the XNR_0417 enzyme, while only the compound 14 was detected in the control strain.

In the case of the rhapontin feeding, the compounds 15, 16, 19 and 20 were detected in the strain *S. albidoflavus* SP43-XNR_0417 and not in the negative control strain. The compound 13 (rhapontin) was not observed in none of the two strains.

Finally, the same compounds 14, 17, 18, 19 and 21 observed in the case of the resveratrol feeding were detected in the extract of the strain *S. albidoflavus*

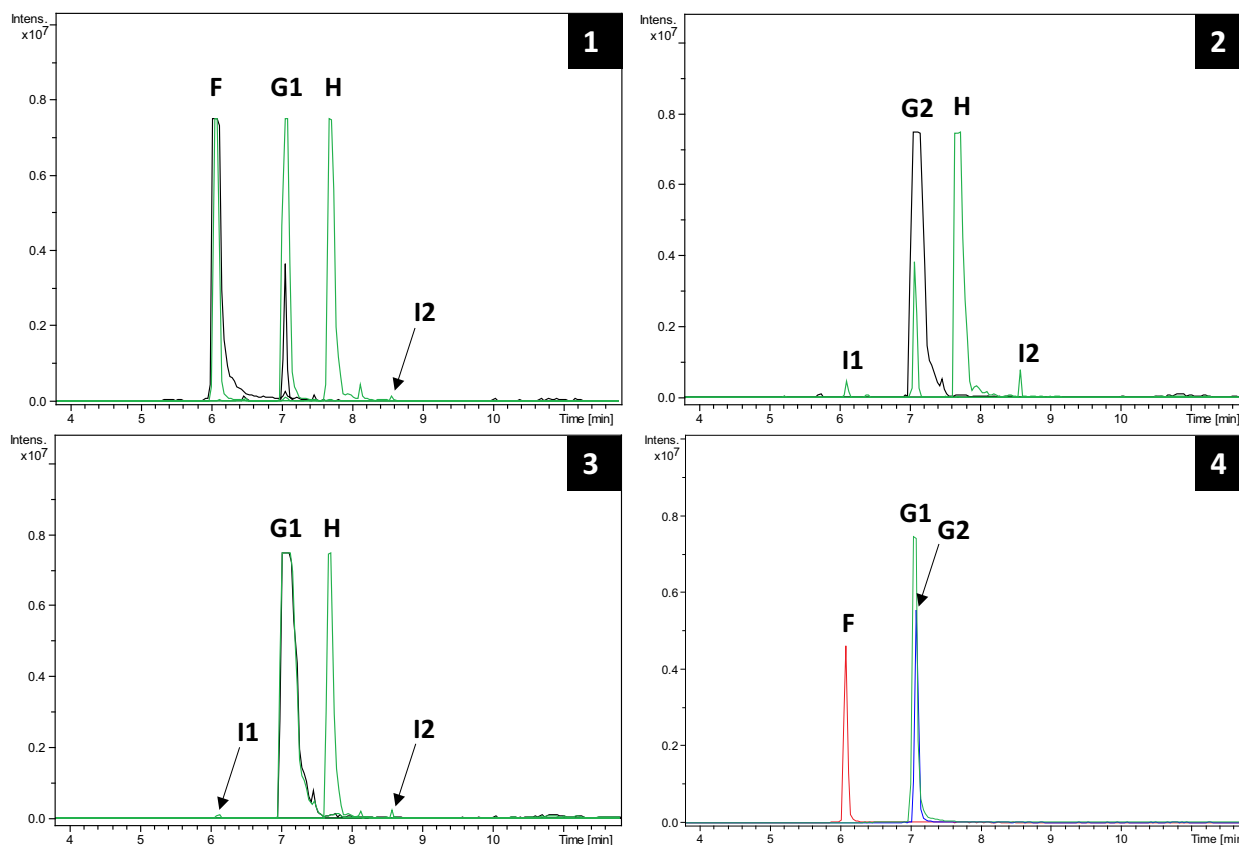


Fig. 7 HPLC–HRESIMS chromatograms of the strains *S. albidoflavus* SP43-XNR_0417 (green) and *S. albidoflavus* ΔXNR_0417 (black) after feeding with the flavones **1** luteolin, **2** diosmetin, and **3** chrysoeriol. **4** Pure standards of luteolin (red, F), diosmetin (blue, G2) and chrysoeriol (green, G1). The capital letters correspond to extracted ion chromatograms (EICs) for different m/z $[M-H]^-$: (F); 285.0404616 (calculated for $C_{15}H_{10}O_6$: flavonoid skeleton without methyl groups), (G1 and G2); 299.0561117 (calculated for $C_{16}H_{12}O_6$: flavonoid skeletons with a total of one methyl group), (H); 313.0717617 (calculated for $C_{17}H_{14}O_6$: flavonoid skeleton with a total of two methyl groups), and (I1 and I2); 327.0874118 (calculated for $C_{18}H_{16}O_6$: flavonoid skeletons with a total of three methyl groups). Capital letters followed by different numbers correspond to different compounds with the same m/z $[M-H]^-$

SP43-XNR_0417 after the polydatin feeding, and only the compound 14 (resveratrol) was detected in the negative control strain. The compound 12 (polydatin) was not observed in any of the two strains. The compounds 15, 16, 17, 18, 19, 20 and 21 remain unknown, and the absence of rhapontin and polydatin in these extracts will be discussed later.

As in the case of the flavonoid feedings, the extracts of the stilbene feedings were analyzed by HPLC–HRESIMS (Fig. 10). After feeding with resveratrol, the signals J (m/z 227.0713678 $[M-H]^-$, calculated for $C_{14}H_{12}O_3$, indicating a stilbene skeleton without methyl groups), K (m/z 241.0870179 $[M-H]^-$, calculated for $C_{15}H_{14}O_3$, indicating a stilbene skeleton with one methyl group) and L (m/z 255.1026679 $[M-H]^-$, calculated for $C_{16}H_{16}O_3$, indicating a stilbene skeleton with two methyl groups) were detected twice in the extract of *S. albidoflavus* SP43-XNR_0417 strain. The signal J was also detected twice in the extract of the negative control strain (Fig. 10(1)).

Also, when the resveratrol pure standard was analyzed by HPLC–HRESIMS, two signals corresponding to J type compounds were detected, with the signal at an earlier retention time being the major one (Fig. 10(1)). These two signals detected after the resveratrol feeding are easily explained due to the trans–cis isomerization of resveratrol that occurs when it is exposed to light between 350 and 450 nm wavelength [38, 39]. All the extractions were carried out under light conditions, unlike the pure standard, which was not exposed to light during a long time. All signals corresponding to resveratrol methylated derivatives were detected as two peaks as well.

In the case of the rhapontin feeding, the signals M (m/z 257.0819325 $[M-H]^-$, calculated for $C_{15}H_{14}O_4$, indicating a stilbene skeleton with one methyl group) and N (m/z 271.0975825 $[M-H]^-$, calculated for $C_{16}H_{16}O_4$, indicating a stilbene skeleton with two methyl groups) were detected twice and the signal O (m/z 285.1132326 $[M-H]^-$, calculated for $C_{17}H_{18}O_4$, indicating a stilbene

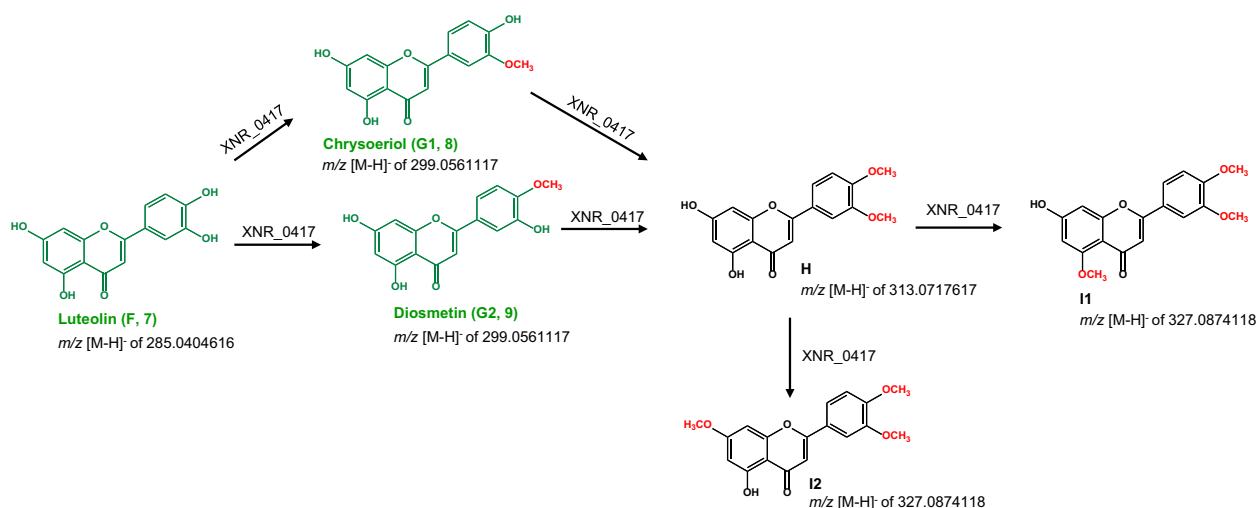


Fig. 8 Proposed compounds generated by the XNR_0417 OMT from the different flavones tested as substrate. Flavones used in the feeding experiments are depicted in green. The *O*-methyl groups introduced by XNR_0417 are highlighted in different color within the structures. Compounds are named as the detected signals of m/z [M-H]⁻ (compounds corroborated with authentic pure standards are also named with their assigned number in the HPLC–DAD analysis)

skeleton with three methyl groups) was detected three times in the strain *S. albidoflavus* SP43-XNR_0417. The signal M was also detected twice in the control strain (Fig. 10(2)), due to the trans–cis photo-isomerization of the rhapontin aglycon (rhapontigenin) [40]. The m/z 419.1347559 [M-H]⁻, calculated for C₂₁H₂₃O₉ and corresponding to rhapontin, was not detected in any of the strains.

Finally, after the polydatin feeding, the signals J, K, and L were detected twice in the strain *S. albidoflavus* SP43-XNR_0417. The signal J was also detected twice in the control strain (Fig. 10(3)). The m/z 389.1241912 [M-H]⁻, calculated for C₂₀H₂₂O₈ and corresponding to polydatin was not detected in any of the strains.

The signal J is resveratrol and corresponds to the compound 14 in Fig. 9. However, only one isomer is detected by HPLC–DAD analysis. The signals K and L have a m/z [M-H]⁻ corresponding to resveratrol methyl ether and resveratrol dimethyl ether, respectively, and they may correspond to some of the unidentified compounds by HPLC–DAD (17, 18, 19 and 21) (Fig. 9C). The different possibilities for the identity of the signals K and L are depicted in Fig. 11. No signals corresponding to resveratrol trimethyl ether were detected.

In the case of the rhapontin feeding, this compound and its methylated derivatives were not detected. However, the signal M, corresponding to rhapontigenin, was detected. Rhapontigenin already harbors a methyl group, and the signals N and O show a m/z [M-H]⁻ like the one of rhapontigenin with one and two extra methyl groups, respectively. These compounds cannot be related with

a specific compound observed by HPLC–DAD analysis (15, 16, 19 and 20) (Fig. 10(2)), but, these signals may correspond to some of them and the possible methyl groups distribution within these compounds is depicted in Fig. 11.

Finally, after the polydatin feeding, this compound and its methylated derivatives were not detected, however, the same signals that in the case of resveratrol feeding (signals J, K and L) were detected. The polydatin aglycon is actually resveratrol, and this result suggests, as in the case of rhapontin, the loss of the sugar moiety during the fermentation. This phenomenon will be addressed in the next section.

In vitro assays to determine the substrate flexibility of XNR_0417 on different flavanones, flavones, and stilbenes

In order to complement the biotransformation experiments previously presented, we carried out in vitro reactions using the pure form of the enzyme XNR_0417 after its expression in *E. coli* and its purification (see “Material and methods” section).

Flavanones

The flavanones hesperetin, eriodictyol, homoeriodictyol and homohesperetin were tested in vitro and analyzed using UPLC–DAD (Fig. 12) and LC–MS (Fig. 13).

After addition of hesperetin to the reaction (Fig. 12A), homohesperetin was obtained as a product, as well as three extra unidentified peaks. Regarding eriodictyol, the purified enzyme generated from this substrate the

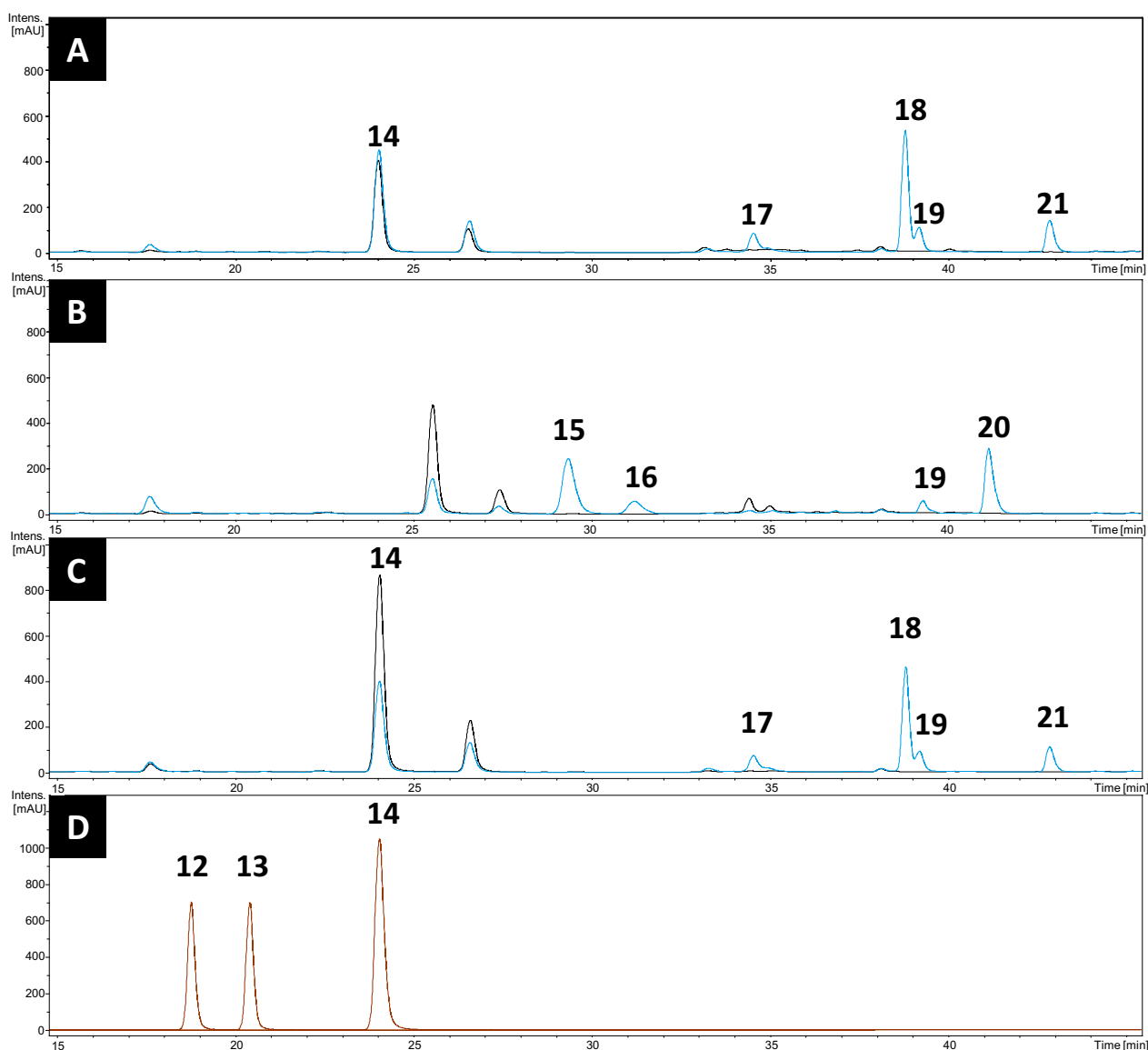


Fig. 9 HPLC–DAD chromatograms of cultures of *S. albidoflavus* Δ XNR_0417 (black) and *S. albidoflavus* SP43-XNR_0417 (blue) after addition of **A** resveratrol 0.1 mM; **B** rhapontin 0.1 mM; and **C** polydatin 0.1 mM. **D** Authentic pure standards of polydatin (**12**), rhapontin (**13**), and resveratrol (**14**). Peaks 15, 16, 17, 18, 19, 20 and 21 are unknown compounds

products homoeriodictyol, homohesperetin and an unidentified compound (Fig. 12B). In the case of homoeriodictyol, homohesperetin was generated, as well as three unidentified compounds (Fig. 12C). Finally, homohesperetin yielded three unidentified products (Fig. 12D). The identification of some of the compounds was carried out using pure standards (Fig. 12E).

These results demonstrate the substrate flexibility of XNR_0417 over flavanone substrates, yielding products with all the compounds tested.

Furthermore, the extracts from the reactions were also analyzed by LC–MS (Fig. 13). In the case of hesperetin, this compound and homohesperetin were detected after the reaction (Fig. 13(1)). In the case of eriodictyol, this compound, homoeriodictyol and homohesperetin were detected (Fig. 13(2)). In the reaction using homoeriodictyol, this compound and homohesperetin were detected (Fig. 13(3)). Finally, in the extract from the reaction using homohesperetin as substrate (Fig. 13(4)) two signals of m/z $[M-H]^-$ of 329.1030618 (calculated for $C_{18}H_{18}O_6$) were detected,

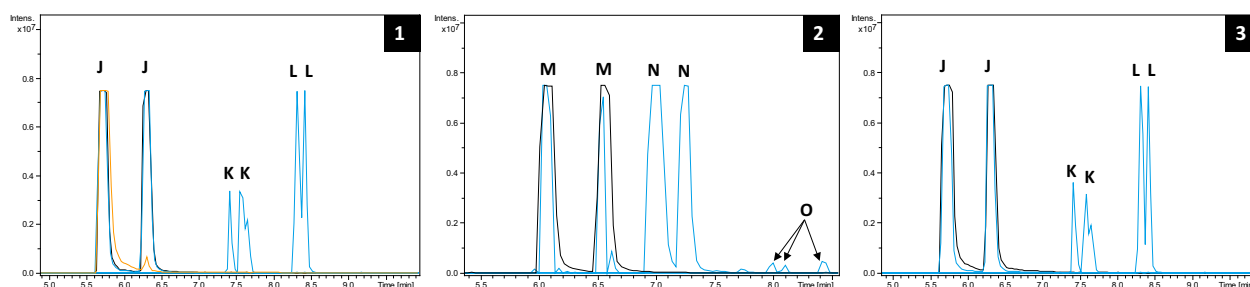


Fig. 10 HPLC–HRESIMS chromatograms of the strains *S. albidoflavus* SP43–XNR_0417 (blue) and *S. albidoflavus* Δ XNR_0417 (black) after feeding with stilbenes **1** resveratrol (pure standard in yellow color), **2** rhapontin, and **3** polydatin. Capital letters correspond to extracted ion chromatograms (EICs) for different m/z $[M-H]^-$: (J); 227.0713678 (calculated for $C_{14}H_{12}O_3$), (K); 241.0870179 (calculated for $C_{15}H_{14}O_3$), (L); 255.1026679 (calculated for $C_{16}H_{16}O_3$), (M); 257.0819325 (calculated for $C_{15}H_{14}O_4$), (N); 271.0975825 (calculated for $C_{16}H_{16}O_4$), and (O); 285.1132326 (calculated for $C_{17}H_{18}O_4$)

however, they are not visible when the EIC of homohesperetin is displayed. Thus, we have included a chromatogram displaying the EIC for the m/z $[M-H]^-$ of 329.1030618 as a supplementary figure (Figure S4). The compounds generated in the reactions were identified using pure standards (Fig. 13(5)).

Flavones

The flavones luteolin, diosmetin and chrysoeriol were tested *in vitro* and analyzed using UPLC–DAD (Fig. 14) and LC–MS (Fig. 15).

After addition of luteolin to the reaction (Fig. 14A), chrysoeriol was obtained as a product, as well as six extra unidentified compounds. Regarding diosmetin (Fig. 14B), seven different unidentified compounds were detected. In the case of chrysoeriol, three unidentified compounds were detected (Fig. 14C). The identification of some of the compounds was carried out using pure standards (Fig. 14D).

These results demonstrate that XNR_0417 is able to take flavones as substrates, yielding products with all the compounds tested.

Additionally, as in the case of flavanones, the extracts from the reactions were also analyzed by LC–MS (Fig. 15). In the case of luteolin, this compound and chrysoeriol were detected, as well as another compound with m/z $[M-H]^-$ of 313.0717617 (signal H, calculated for the dimethylated $C_{17}H_{14}O_6$) (Fig. 15A). After diosmetin feeding, this compound and that corresponding to signal H (calculated for the dimethylated $C_{17}H_{14}O_6$) were detected (Fig. 15(2)). Finally, in the case of chrysoeriol, this compound and compound corresponding to signal H were detected (Fig. 15(3)). Some of these compounds were identified using pure standards (Fig. 15(4)).

Stilbenes

In a similar way that in the case of flavonoids, the stilbenes resveratrol, rhapontin and polydatin were tested *in vitro* and analyzed using UPLC–DAD (Fig. 16) and LC–MS (Fig. 17).

After addition of resveratrol to the reaction (Fig. 16A), four unidentified compounds were detected. Regarding rhapontin (Fig. 16B), nine different unidentified compounds were detected. Finally, six unidentified compounds were detected when polydatin is added as substrate of the reaction (Fig. 16C). The identification of some of the compounds was carried out using pure standards (Fig. 16D).

These results demonstrate that XNR_0417 is able to take not only flavonoids as substrates, but also stilbenes, even if they are glycosylated (rhapontin and polydatin). These three stilbenes yielded different products in presence of the pure *O*-methyltransferase.

The extracts from the reactions with stilbenes were also analyzed by LC–MS (Fig. 17). In the case of resveratrol (Fig. 17(1)), this compound was detected twice (J signals). Also, two signals K $[m/z$ $[M-H]^-$ of 241.0870179 (calculated for $C_{15}H_{14}O_3$), and two signals L $[m/z$ $[M-H]^-$ of 255.1026679 (calculated for $C_{16}H_{16}O_3$) were detected. In the case of rhapontin [signal Y, with m/z $[M-H]^-$ of 419.1348 (calculated for $C_{21}H_{23}O_9$)], two signals M $[m/z$ $[M-H]^-$ of 257.0819325 (calculated for $C_{15}H_{14}O_4$), four signals N $[m/z$ $[M-H]^-$ of 271.0975825 (calculated for $C_{16}H_{16}O_4$) and a signal O $[m/z$ $[M-H]^-$ of 285.1132326 (calculated for $C_{17}H_{18}O_4$) were detected.

Discussion

Few examples of ecological or metabolic relationships between microorganisms and flavonoids are described in the literature, such as the case of apigenin and *Rhizobium* [41], as most microorganisms are not exposed to flavonoids in the environment. The plant-type OMTs are known to transfer methyl groups only to a specific

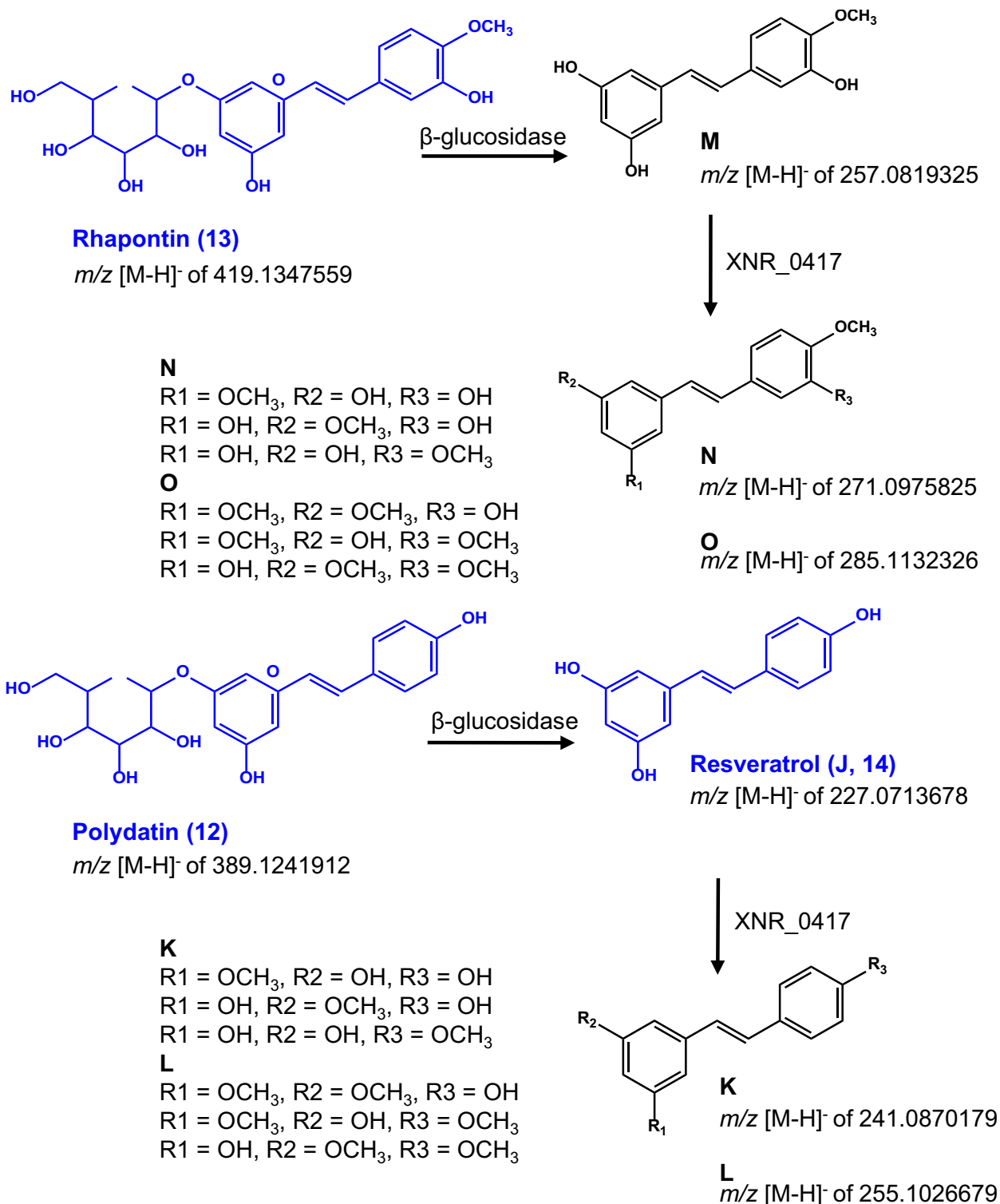


Fig. 11 Proposed compounds generated by the XNR_0417 OMT from the different stilbenes tested as substrate. Stilbenes used in the feeding experiments are depicted in blue. Compounds are named as the detected signals of m/z [M-H]⁻ (compounds corroborated with authentic pure standards are also named with their assigned number in the HPLC-DAD analysis). Compounds containing R in their structures are unknown and can correspond to one of the possible O-methyl groups distribution described next to them

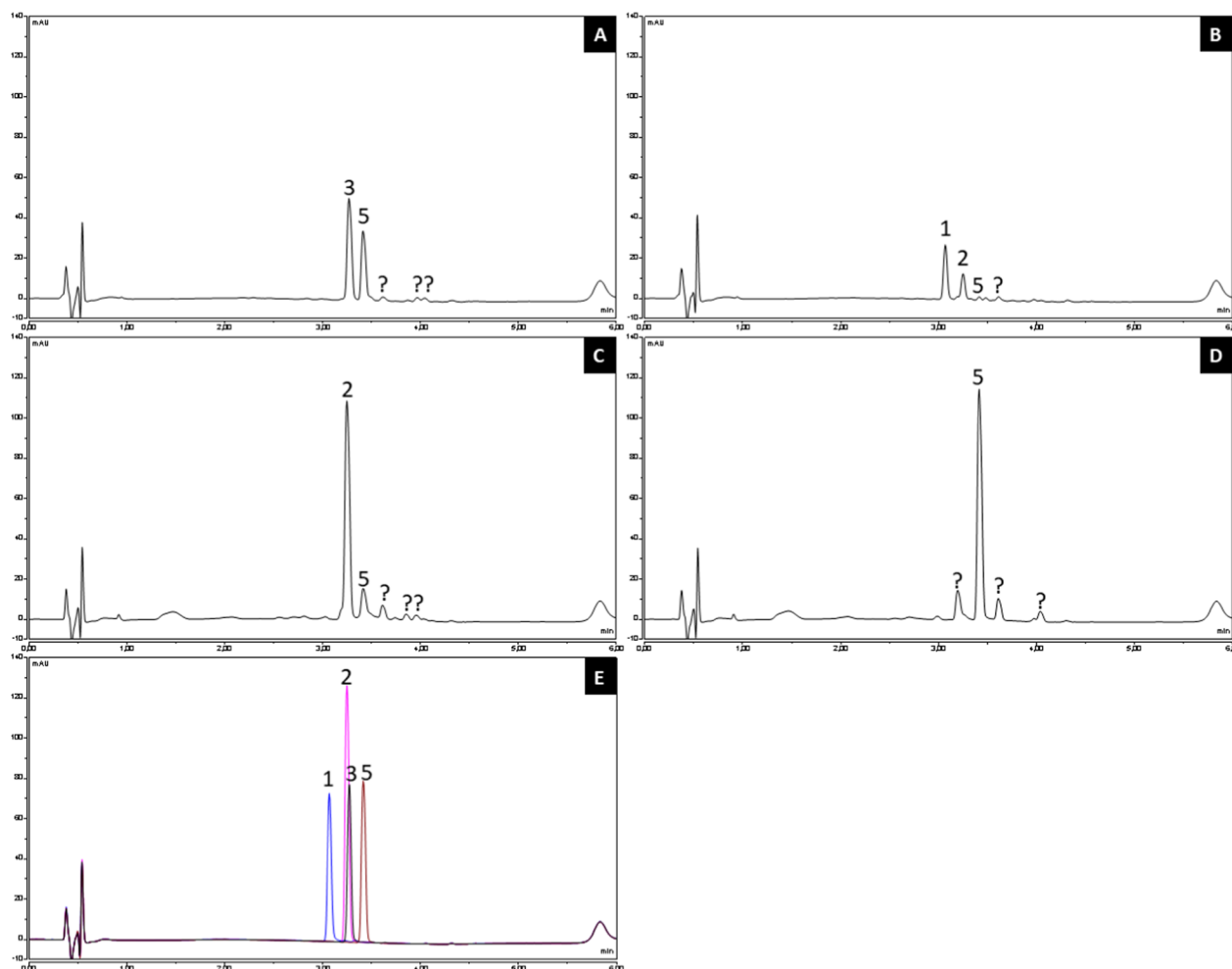


Fig. 12 UPLC–DAD chromatograms of extracts from reactions using XNR_0417 in vitro after addition of **A** hesperetin; **B** eriodictyol; **C** homoeriodictyol; and **D** homoesperetin. **E** Authentic pure standards of eriodictyol (blue, 1), homoeriodictyol (pink, 2), hesperetin (black, 3), and homoesperetin (brown, 5). Unknown peaks (?)

position of a determined substrate [42]. Unlike plants, the functional roles of bacterial OMTs are not well understood and are suggested to increase the antimicrobial activity of some substrates [30]. Several SAM-dependent OMT have been reported from different *Streptomyces* species that have been shown to be involved in the generation of secondary metabolites derivatives [29, 30, 37, 43–48], however, only a few of them are tested and characterized on polyphenolic compounds [28–32].

An OMT from *S. coelicolor* A4(2), ScOMT1, was characterized either in vivo and in vitro, and it recognized *ortho*-dihydroxyflavones, generating mainly mono-methylated derivatives. The common feature among the tested substrates was the existence of two neighboring hydroxyl groups [30]. Another OMT from *S. avermitilis*, SaOMT5, was proven to use different flavonoids as substrates, such as 6,7-dihydroxyflavone, 3',4'-dihydroxyflavone, 7,8-dihydroxyflavone and quercetin. All the substrates

that underwent a reaction yielded only one methylated product and a common feature between them was the presence of two adjacent hydroxyl groups in their structure [29]. More examples of *Streptomyces* possessing flavonoid OMTs are GerMIII from *Streptomyces* sp. KCTC 0041BP, which introduces a methyl group in the 4'-position of the ring B of quercetin and luteolin, with relative conversion rates of 85% and 67%, respectively [31], and SpOMT7740 from *S. peuceitius*, which transfers one, two or three methyl groups to flavones, flavonols or isoflavones, depending on the substrate. However, SpOMT7740 was shown to have low yields [32]. Another interesting OMT from *S. avermitilis* ATCC 31267 (SaOMT2) shows 7-*O*-methylation activity on several flavonoids when expressed in *E. coli*. Interestingly, when SaOMT2 was expressed in *S. venezuelae*, it exhibited more diverse regiospecificity and catalyzed mono-, di-

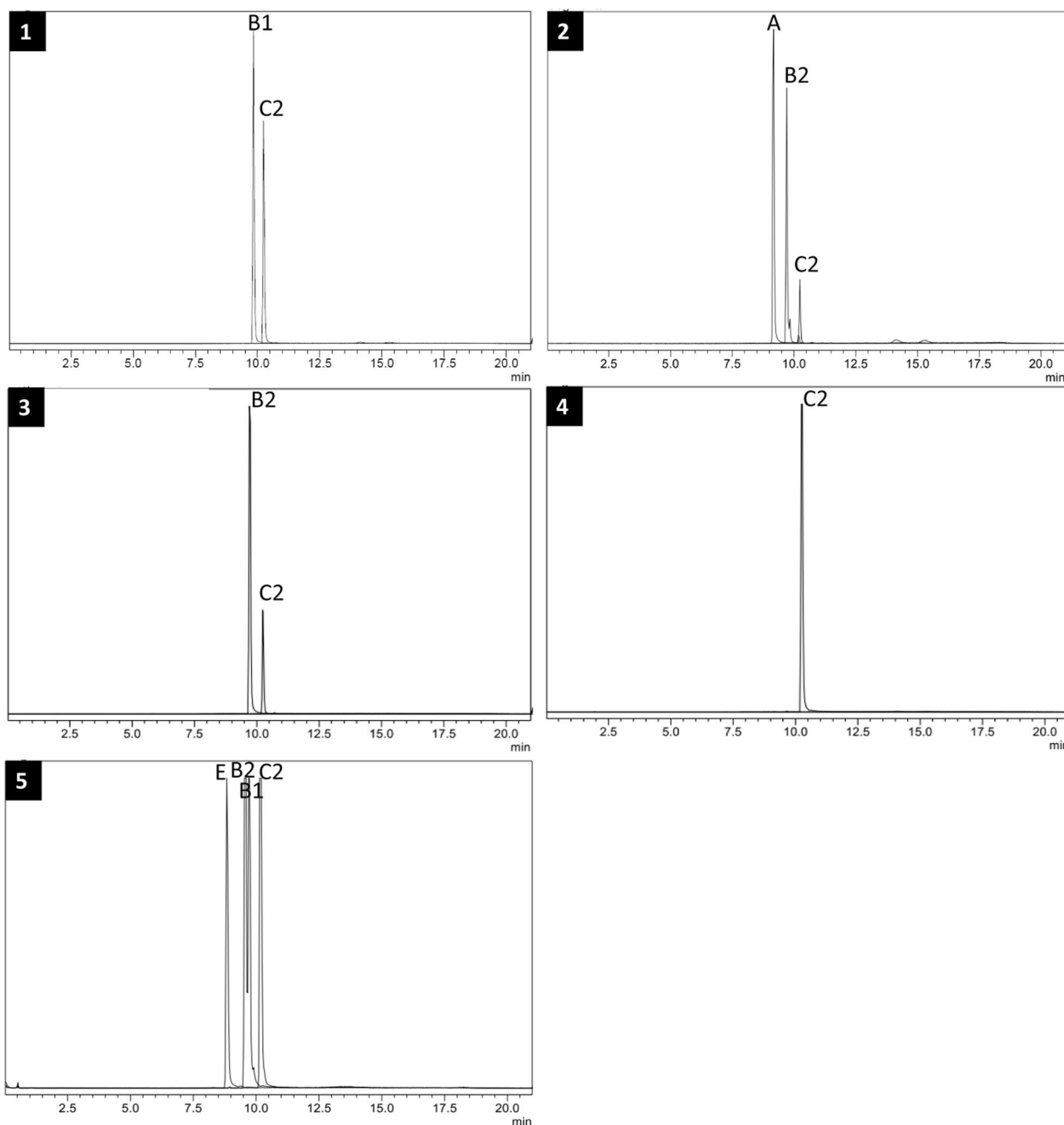


Fig. 13 EICs from LC–MS of extracts from reactions using XNR_0417 in vitro after addition of; **1** hesperetin, **2** eriodictyol, **3** homoeriodictyol and **4** homohesperetin. **5** Pure standards of eriodictyol (E), homoeriodictyol (B2), hesperetin (B1) and homohesperetin (C2). Signal E corresponds to m/z $[M-H]^-$ of 287.0561117 (calculated for $C_{15}H_{12}O_6$), signals B2 and B1 to m/z $[M-H]^-$ of 301.0717617 (calculated for $C_{16}H_{14}O_6$), and signal C2 to m/z $[M-H]^-$ of 315.0874118 (calculated for $C_{17}H_{16}O_6$)

and tri-methylations of flavanones, flavones and stilbenes [28].

In this study we have identified the OMT XNR_0417 of *S. albidoflavus* J1074 as a promising polyphenol OMT and we have proved its broad substrate

flexibility either in vivo and in vitro using the pure enzyme, being this last one able to accept as substrate flavanones, which show a half-chair conformation due to the presence of the dihydropyran ring (ring C) [49], and flavones, possessing an almost planar conformation [50]. These results indicate that may be possible

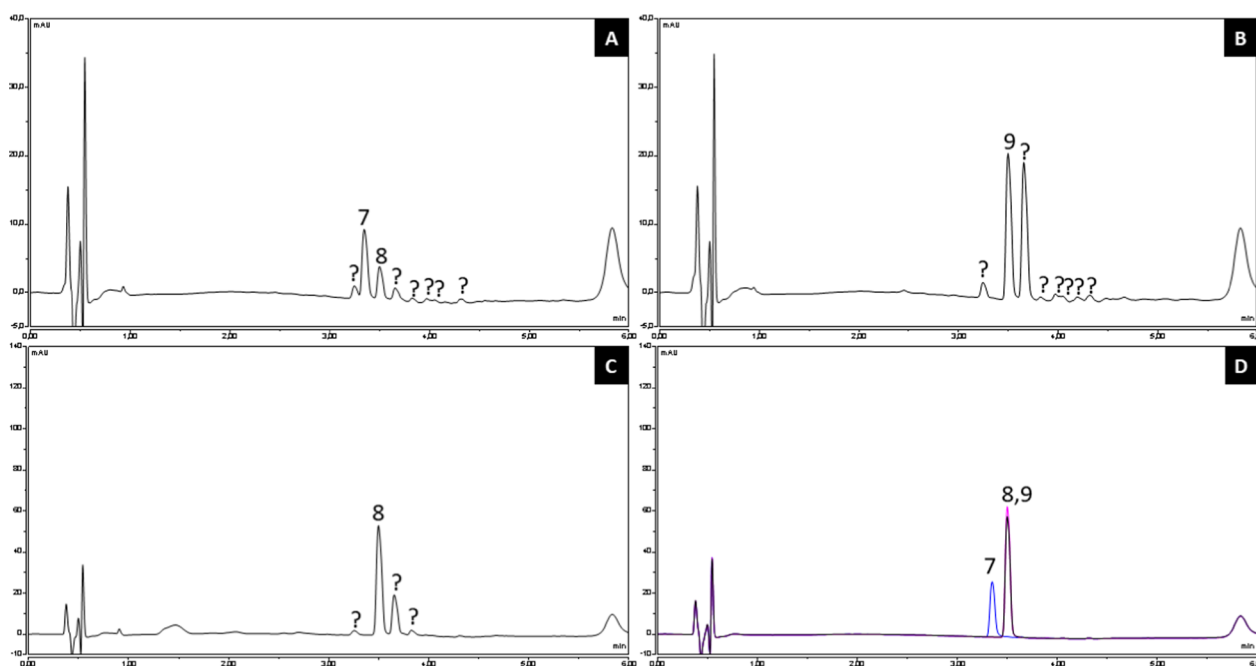


Fig. 14 UPLC–DAD chromatograms of extracts from reactions using XNR_0417 in vitro after addition of **A** luteolin; **B** diosmetin; and **C** chrysoeriol 0.1 mM. **D** Authentic pure standards of luteolin (blue, 7), chrysoeriol (black, 8) and diosmetin (pink, 9). Unknown peaks (?)

the acceptance of other type of flavonoids as substrate, regardless of their spatial configuration.

We have detected mono-, di-, and tri-methylated derivatives of eriodictyol and luteolin, being the mono-methylated ones hesperetin (4'-position), homoeriodictyol (3'-position), diosmetin (4'-position), and chrysoeriol (3'-position). These mono-methylated compounds are also accepted as substrates by XNR_0417, showing a preference for those methylated in the 4' position (hesperetin and diosmetin), since both compounds show a reduction in the extracts at a greater extent than homoeriodictyol and chrysoeriol [both of them methylated in 3' position (Figs. 3 and 6)]. Furthermore, we demonstrated either in vivo and in vitro the acceptance of homohesperetin, a dimethylated flavonoid, as a substrate of XNR_0417.

The *O*-methylation by XNR_0417 in the position 3' of hesperetin and 4' of homoeriodictyol gives rise to the generation of homohesperetin (signal C2, m/z 315.0874118 $[M-H]^-$), which was detected in the extracts of both hesperetin and homoeriodictyol feedings. However, a signal corresponding to a m/z 315.0874118 $[M-H]^-$ (C1) was detected in the homoeriodictyol feeding but not in the hesperetin feeding, which indicates the presence of another di-methylated form of eriodictyol in the extract of homoeriodictyol feeding.

Also, in the case of the eriodictyol feeding, the signals A3 and A4 with a m/z 329.1030618 $[M-H]^-$ were detected, while the same signals were detected in the case

of hesperetin and homoeriodictyol feeding in addition to signals A1 (hesperetin feeding) and A2 (homoeriodictyol and homohesperetin feedings), indicating the presence of different forms of eriodictyol trimethyl ethers.

Furthermore, in the case of the hesperetin, homoeriodictyol and homohesperetin feedings, a signal D, corresponding to the unique possible form of a tetramethylated eriodictyol was detected (m/z 343.1187119 $[M-H]^-$), which would be eriodictyol 5,7,3',4'-tetramethyl ether (compound D in Fig. 5).

On the other hand, regarding the flavones feedings, methylations on the positions 3' and 4' of diosmetin and chrysoeriol respectively gave rise to the generation of luteolin 3',4'-dimethyl ether (m/z 313.0717617 $[M-H]^-$), which was detected in the extracts of luteolin, diosmetin and chrysoeriol feedings.

Also, in the case of the luteolin feeding, the signal I2 (m/z 327.0874118 $[M-H]^-$) was detected, while the signals I1 and I2 were detected in the case of the diosmetin and chrysoeriol feedings. This indicates the presence of one or two forms of luteolin dimethyl ethers, depending on the extract.

The exact determination of the methyl groups in the case of the di-methylated version of eriodictyol found in the homoeriodictyol feeding (signal C1), the tri-methylated versions of eriodictyol found in the hesperetin and homoeriodictyol feedings [A1, A3 and A4 of Fig. 4(1) and A2, A3 and A4 of Fig. 4(3), respectively] and the

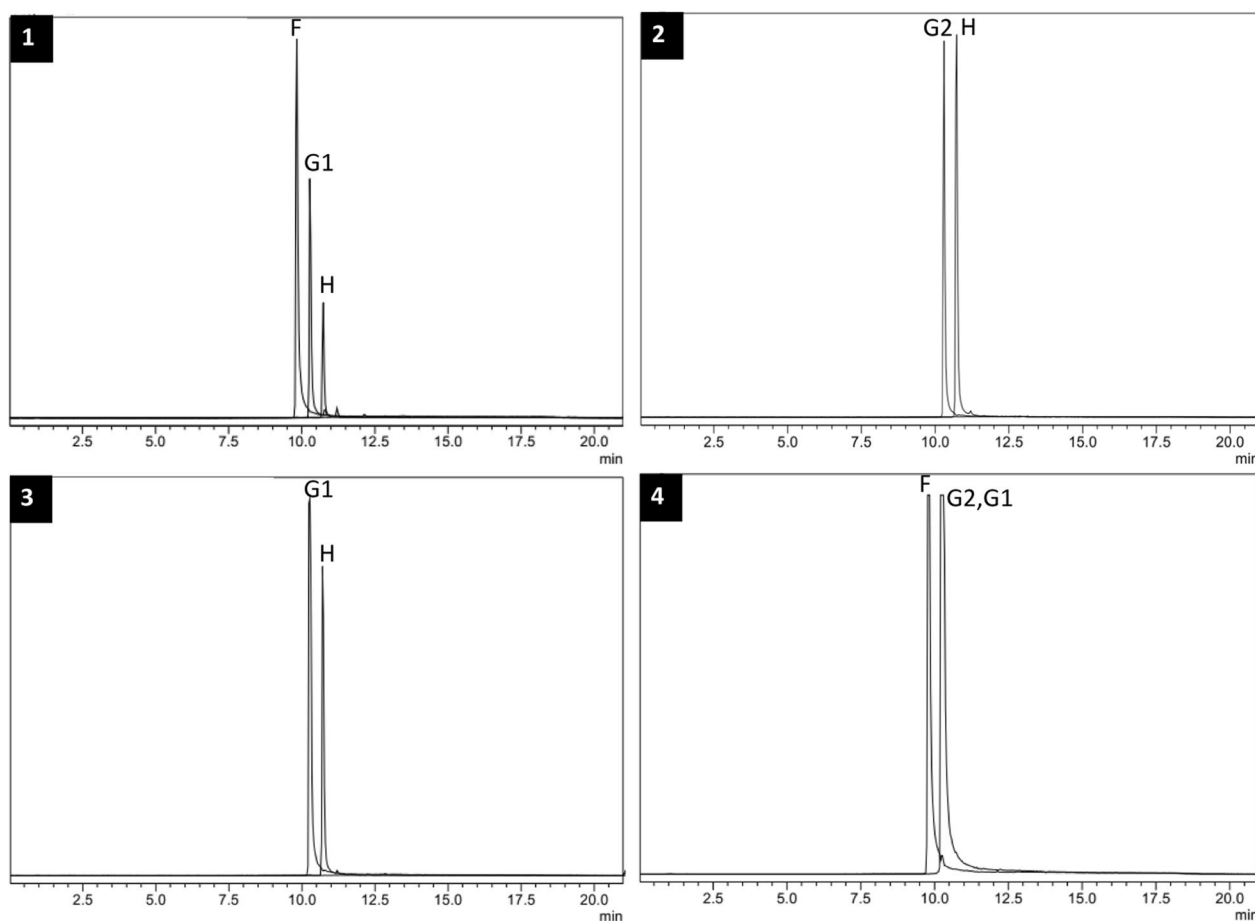


Fig. 15 EICs from LC–MS of extracts from reactions using XNR_0417 in vitro after addition of; **1** luteolin, **2** diosmetin, and **3** chrysoeriol. **4** Pure standards of luteolin (F), diosmetin (G2), and chrysoeriol (G1). Signal F corresponds to m/z $[M-H]^-$ of 285.0404616 (calculated for $C_{15}H_{10}O_6$), signals G2 and G1 to 299.0561117 (calculated for $C_{16}H_{12}O_6$), and signal H to 313.0717617 (calculated for $C_{17}H_{14}O_6$)

tri-methylated versions of luteolin found in the diosmetin and chrysoeriol feedings [signals I1 and I2 in Fig. 7(2, 3)] was not possible.

Although isomeric compounds show a different fragmentation behavior, the exact position of the methyl group cannot be defined using electrospray ionization tandem mass spectrometry (ESI–MS/MS) without nuclear magnetic resonance (NMR) analyses or comparison with pure standards [51]. This impossibility relies on the observation that during the collision induced dissociation spectra of the methylated flavonoids, the loss of the *O*-methyl group takes place with a lower threshold collision energy than all other fragmentation pathways and thus, the fragments specific to given positions of the flavonoid ring system are formed after the loss of the methyl groups [52].

Although methylations increase the hydrophobicity of the flavonoid molecules, the *O*-methylations in position 5 reduce part of the increased hydrophobicity. This effect is explained since the hydroxyl group in position 5 interacts

with the carbonyl group of the C ring through a hydrogen bond. Therefore, when this intramolecular interaction is disrupted after the addition of the methyl group, the carbonyl oxygen is free to interact more with the mobile phase and this decreases its retention time in the chromatography [52]. The analysis of homohesperetin feeding showed that a signal A3 is detected in the HRESIMS chromatogram (Fig. 4D) but peak 4 is not present in the HPLC–DAD chromatogram (Fig. 3D).

Curiously, after homohesperetin feeding, we detected the presence of hesperetin and homoeriodictyol in the extract of the control strain, and only homoeriodictyol in the strain harboring the *O*-methyltransferase [Figure S5, HRESIMS extracted ion chromatograms (EICs)]. These striking results can be explained since *Streptomyces* produces demethylases [53]. Thus, although signals A1 and A2 show the same retention time and homoeriodictyol was detected after homohesperetin feeding in the strain *S. albidoflavus* SP43-XNR_0417 (Figure S5), we hypothesize that signal A1 (Fig. 4(1)) may correspond

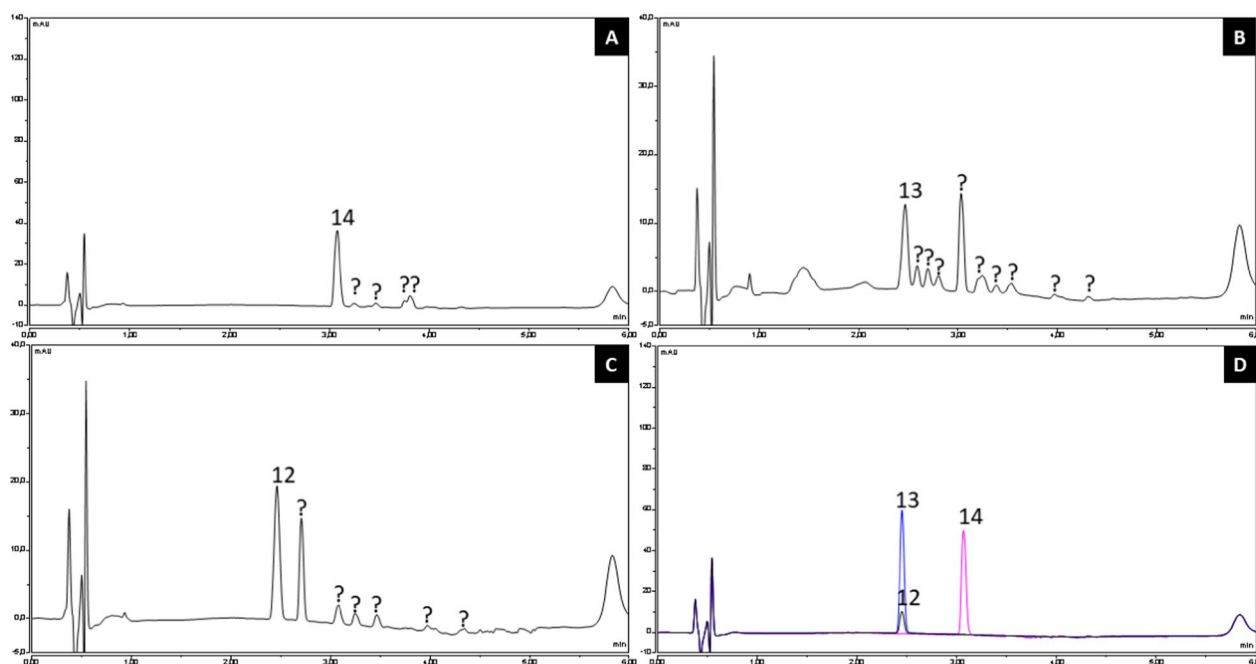


Fig. 16 UPLC–DAD chromatograms of extracts from reactions using XNR_0417 in vitro after addition of **A** resveratrol; **B** rhapontin; and **C** polydatin. **D** Authentic pure standards of polydatin (black, 12), rhapontin (blue, 13) and resveratrol (pink, 14). Unknown peaks (?)

to eriodictyol 5,7,4'-trimethyl ether and the signal A2 (Fig. 4(3)) to eriodictyol 5,7,3'-trimethyl ether. These compounds are a possibility, since no homoeriodictyol (methylated at position 3') was detected in the extract of hesperetin feeding and no hesperetin (methylated at position 4') was detected in the homoeriodictyol feeding, making those two compounds the third possible combination of eriodictyol trimethyl ether for each feeding experiment.

In the case of eriodictyol feeding, the signal A2 should be detectable since homoeriodictyol is present in this extract, however, the peak of this compound was much less intense in the HPLC–DAD chromatogram (Fig. 3B), indicating less amount and thus, the signal A2 is undetectable.

In the case of the two signals with m/z 327.0874118 $[M-H]^-$ (signals I1 and I2) detected in the extract of the strain *S. albidoflavus* SP43-XNR after feedings with diosmetin and chrysoeriol (Fig. 7(2, 3)), the signal I2 (common in the three flavone feedings) could correspond to the peak 11 in Fig. 6, which also appears in all the feedings and may correspond to luteolin 7,3',4'-trimethyl ether: the signal I2 detected by HPLC–HRESIMS appears in a later retention time than the signal I1, which is detected in diosmetin and chrysoeriol feedings (Fig. 7). The signal I1, which is not detected in the luteolin feeding, may correspond to luteolin 5,3',4'-trimethyl ether, following the argument of the *O*-methylated compounds at position 5,

which should elute earlier (see above). However, all these tentative assignments need to be confirmed by NMR or pure standards.

On the other hand, stilbenes are also accepted as substrates of this enzyme. In this case, resveratrol, rhapontin and polydatin were tested as substrates of XNR_0417. Rhapontin and polydatin, which are glycosylated stilbenes, were not possible to be determined as substrates, probably due to the cleavage of the sugar moiety carried out by *Streptomyces albidoflavus* J1074 native enzymes. Bacteria of the genus *Streptomyces* naturally produce β -glucosidases [54–56], and particularly, *Streptomyces albidoflavus* J1074 encodes at least five genes encoding β -glucosidases involved in flavonoids' sugar moieties hydrolysis (<https://www.genome.jp/pathway/salb00946>), which perhaps could also accept stilbenes as substrate. Apparently, the sugar cleavage on stilbene substrates occurs before the action of the methyltransferase XNR_0417. The rhapontin and polydatin aglycones are rhapontigenin (signal M in Fig. 10(2)) and resveratrol (signal J in Fig. 10(3)), respectively, which were detected in the extracts of the strain *S. albidoflavus* SP43-XNR_0417 and the control strain *S. albidoflavus* Δ XNR_0417 after the corresponding feedings.

Rhapontigenin, which already harbors a methyl group at position 4', is substrate of XNR_0417, as the corresponding di-methylated and tri-methylated derivatives

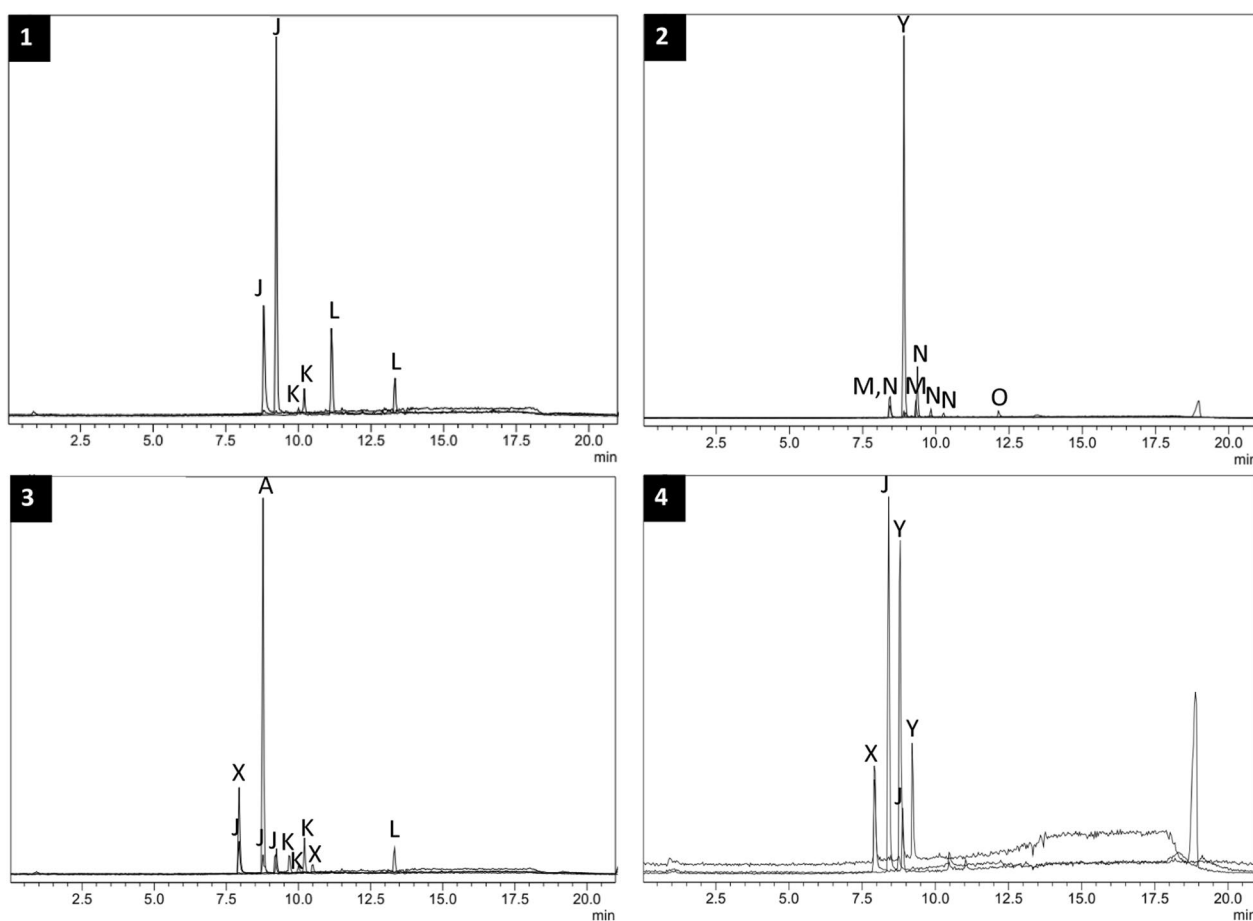


Fig. 17 EICs from LC-MS of extracts from reactions using XNR_0417 in vitro after addition of; **1** resveratrol, **2** rhapontin, and **3** polydatin. **4** Pure standards of polydatin (X), resveratrol (J), and rhapontin (Y). Signal K corresponds to m/z $[M-H]^-$ of 241.0870179 (calculated for $C_{15}H_{14}O_3$), signal L corresponds to m/z $[M-H]^-$ of 255.1026679 (calculated for $C_{16}H_{16}O_3$), signal M corresponds to m/z $[M-H]^-$ of 257.0819325 (calculated for $C_{15}H_{14}O_4$), signal N corresponds to m/z $[M-H]^-$ of 271.0975825 (calculated for $C_{16}H_{16}O_4$), and signal O corresponds to m/z $[M-H]^-$ of 285.1132326 (calculated for $C_{17}H_{18}O_4$)

were detected in the extract of *S. albidoflavus* SP43-XNR_0417 after feeding with rhapontin (Fig. 10(2)).

In the case of the polydatin feeding, its aglycone resveratrol and its corresponding mono-methylated and dimethylated versions were detected (Figs. 9C and 10(3)). Since glycosylated stilbenes cannot be tested as substrate candidates for this *O*-methyltransferase in vivo using *S. albidoflavus* J1074, in vitro assays using the pure enzyme were carried out. After in vitro experiments, we demonstrated that XNR_0417 is able to generate methylated derivatives of the glycosylated stilbenes rhapontin and polydatin. This finding is of particular interest because the presence of bulky moieties in the substrate could induce steric hindrance [57], something which is not taking place with XNR_0417.

Unlike flavonoids, stilbenes backbones isomerize in the presence of light [38, 39]. Since the polyphenol extractions were made under normal laboratory light

conditions and we detected different signals with the same m/z $[M-H]^-$ for each stilbene compound (including their methylated derivatives, in vivo and in vitro), we may be observing trans and cis isomers of each compound in the HPLC-HRESIMS (Fig. 10) and the LC-MS chromatograms (Fig. 17). Possibly, XNR_0417 performs the corresponding *O*-methylations during the fermentation (performed under dark conditions) and these methylated derivatives isomerize during the extraction in the presence of light. If we look at the resveratrol pure standard (Fig. 10(1)), which was not exposed to light for a long time, we observe a main peak corresponding to trans-resveratrol (as specified by the manufacturer), and a small peak that may correspond to cis-resveratrol. However, in contrast to HPLC-HRESIMS and LC-MS, we do not see both isomers in the HPLC-DAD analyses (Fig. 9), probably due to the chromatography column: the HPLC-HRESIMS column particles are more densely packed

compared to those ones in the HPLC–DAD column, and this results in a reduced resolution in the case of HPLC–DAD. However, using UPLC–DAD for the analysis of *in vitro* reactions of stilbenes (Fig. 16), the chromatograms show peaks that may indicate good resolution of the isomers, as observed, for example, in Fig. 16B. Finally, as in the case of some of the tested flavonoids, the exact position of the different methyl groups within the stilbene backbone could not be determined.

Conclusions

OMTs acting on polyphenols during their biosynthesis in their plant natural producers are regiospecific and have strong preference for their natural substrates. The search of microbial enzymes that share homology with plant OMTs can lead to the discovery of potential enzymes with broad substrate flexibility. The enzyme XNR_0417 of *S. albidoflavus* has been shown to be an efficient OMT *in vivo* and *in vitro* on diverse flavanone, flavone and stilbene backbones (and probably also on other polyphenolic backbones), even if these substrates already harbor methyl groups or glucose in their structures. Therefore, the enzyme XNR_0417 is able to generate a variety of methylated derivatives at different OH positions, depending on the initial compound, which makes this enzyme interesting for pharmaceutical purposes at industrial scale. On the other hand, the exact position of the methyl groups in some of the compounds generated by XNR_0417 could not be assigned by HPLC–HRESIMS, and in these cases, new pure standards or NMR studies will be needed.

Material and methods

Reagents and biochemicals

All solvents used for solid phase extraction and HPLC–DAD analysis were LC–MS grade from either Sigma-Aldrich (Madrid, Spain) or VWR Chemicals (Barcelona, Spain) or Merck KGaG (Darmstadt, Germany). All pure flavonoids and stilbenes used in this study were provided by Extrasynthese (Genay, France) or were purchased from Sigma-Aldrich (St Luis, USA). PCR BIO Ladder II (Sursee, Switzerland) was used in agarose gels.

Primers and enzymes

Restriction enzymes and T4 DNA ligase were purchased from Thermo Fisher Scientific (Madrid, Spain) or New England BioLabs (Ipswich, MA, USA). Herculase II Fusion DNA polymerase was purchased from Agilent Technologies (Madrid, Spain), Terra PCR Direct polymerase from Takara (London, United Kingdom), and NEBuilder® HiFi DNA Assembly Master Mix from New England BioLabs (Ipswich, MA, USA). The primers used for the generation and confirmation of the strains used in

this study are listed in Table S1 (IDT Technologies, Brussels, Belgium, or Thermo Fisher Scientific, MA, USA).

Bacterial strains and culture conditions

All strains in this study are listed in Table 1. *Escherichia coli* TOP10 (Invitrogen, Madrid, Spain) was used for routine subcloning. *E. coli* ET12567/pUZ8002 [58] was used for conjugation. *E. coli* DH5 α was used for cloning and maintenance, *E. coli* BL21 (DE3) was used for enzyme expression (New England BioLabs, Ipswich, MA, USA). The *S. albidoflavus* strains used in this work have been generated by bacterial conjugation. The new strains were confirmed by antibiotic resistance and, in the case of the chromosomal deletion, by polymerase chain reaction (PCR).

The strains used in this study are *S. albidoflavus* J1074, *S. albidoflavus* Δ XNR_0417 and *S. albidoflavus* SP43-XNR_0417. *S. albidoflavus* Δ XNR_0417 is a mutant strain of *S. albidoflavus* J1074 in the gene XNR_0417 and was generated using the CRISPR-Cas9 based plasmid pSEVAUO-C41012-XNR_0417. On the other hand, the strain *S. albidoflavus* SP43-XNR_0417 was generated using the plasmid pSEVAUO-M21402-XNR_0417, which was integrated into the Φ BT1 *attB* site of the chromosome of *S. albidoflavus* Δ XNR_0417.

E. coli strains were grown in tryptic soy broth (TSB, VWR, Barcelona, Spain) or on TSB agar plates, supplemented with the corresponding antibiotic (apramycin 100 μ g/mL, Thermo Fisher Scientific, Madrid, Spain), kanamycin 100 μ g/mL (Alfa Aesar, Ward hill, MA, USA), chloramphenicol 25 μ g/mL (AppliChem, Darmstadt, Germany), nalidixic acid 50 μ g/mL (Acros Organics, Brussels, Belgium) and X-gal (AppliChem, Darmstadt, Germany) when blue-white selection is needed. *S. albidoflavus* was grown at 30 °C on Bennet medium, supplemented with the corresponding antibiotics when necessary (thiostrepton 50 μ g/mL or apramycin 50 μ g/mL, Cayman Chemical, Ann Arbor, MI, USA) for sporulation [61]. For feeding experiments, *S. albidoflavus* spores were quantified, and an inoculum of 10⁶ spores/mL was performed in triplicate in flasks with 25 mL of NL333 medium and incubated during 120 h at 30 °C and 250 rpm. Flavonoids and stilbenes were added to the medium 24 h after starting cultivation, at 0.1 mM final concentration.

Transformed *E. coli* strains were grown at 37 °C in lysogeny broth (LB, Sigma-Aldrich, St. Louis, USA) or on LB agar plates supplemented with 30 μ g/mL kanamycin and 20 μ g/mL X-gal (Cayman Chemical Company, Ann Arbor, MI, USA) for blue-white selection. To purify the recombinant protein, *E. coli* BL21 (DE3) strains were cultured in 500 mL of liquid Dynamite Medium [62] inoculated with 1% (v/v) of overnight preculture and

Table 1 Plasmids and strains used in this study

Plasmids	Description	Source
pSEVA88c1	Replicative shuttle vector	[58]
pSEVA88c1-XNR_0417	pSEVA88c1 harboring homologous arms for XNR_0417 knock out generation	This study
pSEVAUO-C41012	Replicative shuttle vector harboring the nuclease cas9	[57]
pSEVAUO-C41012-Spacer-XNR_0417	pSEVAUO-C41012 harboring the spacer for BGC20 deletion	This study
pSEVAUO-C41012-XNR_0417	pSEVAUO-C41012-Spacer-BGC20 harboring homologous arms for BGC20 deletion	This study
PCR-Blunt II-TOPO	Replicative blunt DNA cloning vector	Invitrogen
PCR-Blunt II-TOPO-XNR_0417	PCR-Blunt II-TOPO harboring <i>XNR_0417</i>	This study
pSEVA181SP43	Source of <i>SP43</i> (level 0 MoClo)	EXPLORA
pSEVA181RiboJ-RBS	Source of <i>RiboJ-RBS</i> (level 0 MoClo)	EXPLORA
pIDTSMARTttsbib	Source of <i>ttsbib</i> (level 0 MoClo)	IDT
pSEVAUO-M21402-XNR_0417	Level 1 MoClo plasmid harboring <i>XNR_0417</i>	This study
pTrc_12	pSEVA23g19g2, pUC ori, KmR, <i>lacI</i> , <i>trc</i> promoter, T7 terminator	[59]
pTrc-XNR_0417	pTrc harboring XNR_0417, N-6xHis—level 1 MoClo	This study
Strains		
<i>E. coli</i> TOP10	Strain used for routine subcloning	Invitrogen
<i>E. coli</i> ET12567/pUZ8002	Strain used for conjugation	[55]
<i>S. albidoflavus</i> J1074	<i>S. albidoflavus</i> mutant of the <i>S. albidoflavus</i> G strain that lacks an active <i>Sall</i> restriction modification system	[60]
<i>E. coli</i> DH5-alpha	F' proA ⁺ B ⁺ lacI ^q Δ(lacZ)M15 zff::Tn10 (Tet ^R)/fhuA2Δ(argF-lacZ)U169 phoA glnV44 Φ80Δ(lacZ)M15 gyrA96 recA1 relA1 endA1 thi-1 hsdR17	New England Biolabs
<i>E. coli</i> BL21 (DE3)	fhuA2 [lon] ompT gal (λ DE3) [dcm] ΔhsdS, λ DE3 = λ sBamHlo ΔEcoRI-B int::[lacI:PlacUV5::T7 gene1] i21 Δnin5	New England Biolabs
<i>S. albidoflavus</i> ΔXNR_0417	<i>S. albidoflavus</i> mutant strain for the gene <i>XNR_0417</i>	This study
<i>S. albidoflavus</i> SP43-XNR_0417	<i>S. albidoflavus</i> strain harboring the gene <i>XNR_0417</i> under the control of <i>SP43</i>	This study

supplemented with kanamycin (30 µg/mL). Cultures were initially incubated at 37 °C with 120 rpm agitation until the optimal density at 600 nm (OD₆₀₀) reached 0.6. Protein expression was then induced by the addition of 0.5 mM IPTG (isopropyl β-D-1-thiogalactopyranoside, Sigma-Aldrich, St. Louis, USA) and was maintained at 25 °C for 20 h.

Protein purification

The culture cells were harvested and washed according to a previously described protocol [63]. For disruption, cells were incubated with 0.6 mg/mL lysozyme (Sigma-Aldrich, St. Louis, USA) and 25 U/mL viscolase (A&A Biotechnology, Gdańsk, Poland), at 4 °C for 1 h and sonicated on ice for 6 min according to the following procedure—30 s pulses and 30 s pauses at 85% amplitude (Vibra-Cell Ultrasonic Liquid Processor VCX 130, Materials, Newtown, USA). The filtered cell extract was applied to a 5-mL IMAC HisTrap TM HP column (GE Healthcare), following the standard purification procedure using Tris–HCl buffer (pH 7.4, 20 mM, containing 0.5 M NaCl, and 15 mM imidazole for binding and 500 mM for elution). Purified enzyme fractions were stored at 4 °C or used immediately after purification.

Protein concentration was determined by the Bradford assay [64] using a spectrophotometer (Eppendorf Bio-Spectrometer Kinetic) and bovine serum albumin as a reference for the calibration curve. Protein purification was evaluated via 10% SDS-PAGE electrophoresis (BIO-RAD, Hercules, CA, USA) (Figure S6), proteins were stained by Coomassie Brilliant Blue (Cepham Life Sciences, Inc) and Precision Plus Protein Dual Color Standard (BIO-RAD, Hercules, CA, USA) was used as a size marker.

In vitro reaction assay

The standard in vitro activity assay [0.05 mM substrate, 0.5 mM *S*-Adenosyl-L-Methionine (SAM), 20 µL purified enzyme fraction (8.3 mg/mL)] was carried out in 30 mM Tris–HCl buffer (pH 8, 5 mM MgCl₂) at 30 °C, 800 rpm for 67 h. Reactions were stopped by the addition of 200 µL ethyl acetate, vortexed, centrifuged (21,000×g, 5 min), and 20 µL of an organic fraction was transferred to 180 µL of methanol and analyzed by UPLC–DAD liquid chromatography and LC–MS analysis.

Plasmids construction

All the plasmids used in this study are listed in Table 1.

Construction of pSEVAUO-C41012-XNR_0417

To generate a CRISPR-Cas9 based plasmid for the deletion of the gene XNR_0417 in the chromosome of *S. albidoflavus* J1074, a protospacer of 20 bp was designed and cloned into the pSEVAUO-C41012 vector [65] through a Golden Gate reaction, giving rise to pSEVAUO-C41012-Spacer-XNR_0417 (chromosomal position 499,932–499,951).

Two homologous arms interrupting the gene XNR_0417 at the beginning and at the end were amplified from the *S. albidoflavus* J1074 genome using HerculesII Fusion DNA polymerase (Agilent, Madrid, Spain) and cloned into the pSEVA88c1 vector [66] by Gibson assembly, giving rise to pSEVA88c1-XNR_0417 (the flanking homologous arms include chromosomal regions 497,516–499,362 and 500,223–502,108). The corresponding homologous arms were then cloned into the plasmid pSEVAUO-C41012-Spacer-XNR_0417 using the restriction enzymes *PacI* and *SpeI* and the T4 DNA ligase (Thermo Fisher, Madrid, Spain), leading to the generation of the final plasmid pSEVAUO-C41012-XNR_0417.

Construction of pSEVAUO-M21402-XNR_0417

The gene XNR_0417 was PCR amplified from the chromosome of *S. albidoflavus* J1074 using the primers “XNR_0417 fw” and “XNR_0417 rev” (Table S1). The amplicon was cloned into the PCR-Blunt II-TOPO vector (Thermo Fisher Scientific, Madrid, Spain), giving rise the plasmid PCR-Blunt II-TOPO-XNR_0417. The plasmid pSEVAUO-M21402-XNR_0417 was assembled in a level 1 MoClo reaction from the level 0 plasmids pSEVA181SP43, pSEVA181RiboJ-RBS, pIDTSMART-ttsbib [65], PCR-Blunt II-TOPO-XNR_0417 (this study) and the level 1 receptor pSEVAUO-M21402 [65].

Construction of pTrc-XNR_0417

Codon-optimized sequence (ORF) encoding XNR_0417 flanked by *BsaI* restriction sites was purchased from Gen Art (Fisher Scientific, MA, USA) and inserted into the pTrc_12 vector [59] according to the Golden Standard Modular Cloning System (GS MoClo) [67]. The primers sequences used in this study can be found in Table S1. Genetic constructs were verified by sequencing (Macrogen Europe, The Netherlands).

Polyphenol extraction, HPLC–DAD and HPLC–HRESIMS analyses

Spores from *S. albidoflavus* strains were incubated as described before in NL333 culture medium (10^6 spores/mL). Polyphenols were obtained using an organic extraction with acetone (cellular pellet) and ethyl acetate (culture supernatant) [34].

For the identification of polyphenols using HPLC–DAD, the final dry extract obtained from each cultivation condition was dissolved in 100 μ L DMSO/MeOH 1:1 (v/v), and the samples were centrifuged prior to the injection in the equipment. The HPLC separation was performed as described in [34].

For the identification of polyphenols using HPLC–HRESIMS, the dry extract obtained was reconstituted in 200 μ L DMSO/MeOH 1:1 (v/v), and the samples were processed sequentially through 0.8 and 0.2 μ m filters (Acrodisc, Pall, Port Washington, NY, USA). Separation was performed in a UPLC system (Dionex Ultimate 3000, ThermoScientific, Madrid, Spain) equipped with an analytical RP-18 HPLC column (50 \times 2.1 mm, Zorbax® Eclipse Plus, 1.8 μ m, Agilent Technologies, Madrid, Spain) heated to 30 °C, and a combination of distilled water (mobile phase A) and MeCN (mobile phase B), both acidified with 0.1% (v/v) of formic acid, was used. The analytes were eluted at a flow rate of 0.25 mL/min in a 10–100% (v/v) gradient of MeCN under the following conditions: 0–1 min (10% B), 1–4 min (10–35% B), 4–5 min (35% B), 5–8 min (35–100% B), 8–10 min (100% B), 10–11 min (100–10% B) and 11–15 min (10% B). The column effluent was directed to electrospray ionization mass spectrometry analysis (HPLC–ESI–MS) using an ESI-UHR-Qq-TOF Impact II spectrometer (Bruker España SA, Madrid, Spain) which acquired data in the negative ion mode, with a *m/z* range from 40 to 2000 Da. Data were analyzed using Compass DataAnalysis 4.3 (Bruker). The obtained BPCs were extracted for the deprotonated ions of a set of polyphenols with a mass error range of 0.005 mmu (milli mass units), and the obtained EICs were compared with authentic commercial standards, when possible.

UPLC–DAD analysis was performed on an Ultimate 3000 chromatograph (Dionex, Sunnyvale, CA, USA) equipped with a DPG-3600A dual pump liquid control module and diode array detector. LC–MS analysis was performed on a LC–MS 8045 SHIMADZU (SHIM-POL A.M. Borzymowski, Warsaw, Poland). All analysis were carried out according to the procedure described previously [63].

LC–MS analysis was performed on a LC–MS 8045 SHIMADZU (SHIM-POL A.M. Borzymowski, Warsaw, Poland) equipped with a triple quadrupole, and diode array detector. Kinetex column C18 (3 \times 100 mm, 2.6 μ m

100 Å, Phenomenex, Torrance, CA, USA) equipped with a pre-column. The mobile phase was a mixture of water with 0.01% formic acid v/v (A) and methanol (B). The flow rate was 0.3 mL/min, and the column temperature was 40 °C. The nebulizing gas flow: 3 L/min, heating gas flow: 10 L/min, interface temperature: 300 °C, drying gas flow: 10 L/min, data acquisition range m/z 100–800 Da, ionization mode—positive and negative.

Phylogenetic analysis

The phylogenetic tree was performed using the ClustalW program for multiple sequence alignment from the EMBL-EBI (<https://www.ebi.ac.uk/jdispatcher/msa/clustalo>). The code obtained for the tree was used to generate the Figure S1 in the iTOL platform (<https://itol.embl.de/>).

Supplementary Information

The online version contains supplementary material available at <https://doi.org/10.1186/s12934-024-02541-8>.

Figure S1. Phylogenetic tree generated from amino acid sequences of flavonoid OMTs from plants (green color) and *Streptomyces* (yellow color). Those sequences in blue color are OMTs from bacteriophages. The employed sequences for the analysis belong to the following organisms: *Streptomyces* phage Austintatious (QAX92785.1); *Bacteriophage* sp. (UVM85936.1); *Bacteriophage* sp. (UWI10895.1); *Bacteriophage* sp. (UWI13405.1); *Streptomyces* sp. KCTC 0041BP (GermIII); *Arabidopsis thaliana* (At4g26220); *Streptomyces* phage Kradal (QBZ71914.1); *Streptomyces peucetius* (SpOMT7740); *Streptomyces avermitilis* (SaOMT2); *Streptomyces albidoflavus* J1074 (XNR_0417); *Streptomyces coelicolor* A4(2) (ScOMT1); *Glycine max* (SOMT-2); *Plagiochasma appendiculatum* (Pa4'OMT); *Oryza sativa* (OsNOMT and NP_001390411.1); *Zea mays* (NP_001106047.1).

Figure S2. Generation of the *S. albidoflavus* ΔXNR_0417 strain. A) Agarose gel for PCR verification of the XNR_0417 knock out event using the primers "D0417 check fw" and "D0417 check rev". Lanes 1 to 5 are different clones of the strain *S. albidoflavus* ΔXNR_0417, while C is the parental strain *S. albidoflavus* J1074. The size of the expected band in the mutant strain is 2062 bp, while in the control strain is 2926 bp. B) Graphical representation of the expected PCR amplifications shown in the agarose gel picture either in the control strain *S. albidoflavus* J1074 and in the mutant strain *S. albidoflavus* ΔXNR_0417. UNS8: noncoding DNA region of 40 bp, cloned in the pSEVAUO-C41012-XNR_0417 plasmid between the homologous arms.

Figure S3. A) HPLC–DAD chromatograms of *S. albidoflavus* SP43-XNR_0417 with hesperetin feeding (red) and *S. albidoflavus* SP43-XNR_0417 with homoeriodictyol feeding (blue). B) Absorption spectrum of peak 2'. C) Absorption spectrum of peak 2 (homoeriodictyol).

Figure S4. EIC of the m/z [M–H][−]: 329.1030618 (calculated for C₁₈H₁₈O₆) from LC–MS of the extract from the reaction using XNR_0417 in vitro after addition of homoheperetin.

Figure S5. EICs from HPLC–HRESIMS for m/z [M–H][−]: 301.0717617 (calculated for C₁₆H₁₄O₆). A) Extract from *S. albidoflavus* ΔXNR_0417. B) Extract from *S. albidoflavus* SP43-XNR_0417. C) Hesperetin pure standard. D) Homoeriodictyol pure standard.

Figure S6. SDS-PAGE gel electrophoresis of recombinant O-methyltransferase XNR_0417: ladder (line1), crude (line 2), filtrate (line 3), wash (line4), collected fractions of enzyme (line 5–11). Expected mass of purified XNR_0417 fraction: 37.4 kDa. PageRuler™ Plus Prestained Protein Ladder (Thermo Fisher Scientific, MA, USA).

Supplementary Material 7.

Acknowledgements

Authors thank the Mass Spectrometry Unit of the *Servicios Científico-Técnicos* at the University of Oviedo.

Author contributions

Funding acquisition (F.L.), investigation (A.P-V, P.M-C, K.D, A.M., J.P, S.Y.); Supervision (E.H, C.V., F.L.); writing—original draft (A.P-V); writing—review and editing (A.P-V, S.Y, F.L.).

Funding

This research was funded by Principado de Asturias (Spain) through the program "Ayudas a organismos públicos para apoyar las actividades de I+D+I de sus grupos de investigación" (Grant AYUD/2021/51347), as well as by "Programa Severo Ochoa de Ayudas Predoctorales para la investigación y docencia" from Principado de Asturias (Grant PA-20-PF-BP19-058 to PMC and Grant PA-21-PF-BP20-150 to APV), the research project PID2021-127812OB-I00 from MICINN (Spanish Ministry of Science and Innovation), the European Union's Horizon 2020 Research and Innovation Program under Grant Agreement no. 814650 for the project SynBio4Flav, and the Polish National Agency for Academic Exchange under the STER Internationalisation of Doctoral Schools programme under the contract no. BPI/STER/2021/1/00008/U/00001 International Interdisciplinary Doctoral School—at the HEART of BioBased University (I2PhD@BBUniHEART).

Availability of data and materials

Data and materials can be obtained from the research group upon request. Sequences accession data have been included in "Material and methods" section.

Declarations

Ethics approval and consent to participate

Not applicable.

Consent for publication

All authors have read and approved the final version of the manuscript and have accepted its publication in this journal.

Competing interests

The authors declare no competing interests.

Received: 17 June 2024 Accepted: 26 September 2024

Published online: 05 October 2024

References

- Tsao R. Chemistry and biochemistry of dietary polyphenols. *Nutrients*. 2010;2:1231–46.
- Manach C, Scalbert A, Morand C, Rémésy C, Jiménez L. Polyphenols: food sources and bioavailability. *Am J Clin Nutr*. 2004;79:727–47.
- Chaudhuri S, Sengupta B, Taylor J, Pahari BP, Sengupta PK. Interactions of dietary flavonoids with proteins: insights from fluorescence spectroscopy and other related biophysical studies. *Curr Drug Metab*. 2013;14:491–503.
- González-Vallinas M, González-Castejón M, Rodríguez-Casado A, Ramírez de Molina A. Dietary phytochemicals in cancer prevention and therapy: a complementary approach with promising perspectives. *Nutr Rev*. 2013;71:585–99.
- Li A-N, Li S, Zhang Y-J, Xu X-R, Chen Y-M, Li H-B. Resources and biological activities of natural polyphenols. *Nutrients*. 2014;6:6020–47.
- Wang R, Lenka SK, Kumar V, Sikron-Persi N, Dynkin I, Weiss D, et al. A synchronized increase of stilbenes and flavonoids in metabolically engineered *Vitis vinifera* cv. Gamay red cell culture. *J Agric Food Chem*. 2021;69:7922–31.
- Al-Khayri JM, Mascarenhas R, Harish HM, Gowda Y, Lakshmaiah VV, Nagella P, et al. Stilbenes, a versatile class of natural metabolites for inflammation—an overview. *Molecules*. 2023;28:1–28.

8. Ravishankar D, Rajora AK, Greco F, Osborn HMI. Flavonoids as prospective compounds for anti-cancer therapy. *Int J Biochem Cell Biol*. 2013;45:2821–31.
9. Yao B, Fang H, Xu W, Yan Y, Xu H, Liu Y, et al. Dietary fiber intake and risk of type 2 diabetes: a dose-response analysis of prospective studies. *Eur J Epidemiol*. 2014;29:79–88.
10. Nagumo M, Ninomiya M, Oshima N, Itoh T, Tanaka K, Nishina A, et al. Comparative analysis of stilbene and benzofuran neolignan derivatives as acetylcholinesterase inhibitors with neuroprotective and anti-inflammatory activities. *Bioorg Med Chem Lett*. 2019;29:2475–9.
11. Zhao K, Yuan Y, Lin B, Miao Z, Li Z, Guo Q, et al. LW-215, a newly synthesized flavonoid, exhibits potent anti-angiogenic activity in vitro and in vivo. *Gene*. 2018;642:533–41.
12. Camero CM, Germanò MP, Rapisarda A, D'Angelo V, Amira S, Benchikh F, et al. Anti-angiogenic activity of iridoids from *Galium tunetanum*. *Rev Bras Farmacogn*. 2018;28:374–7.
13. Zhao L, Yuan X, Wang J, Feng Y, Ji F, Li Z, et al. A review on flavones targeting serine/threonine protein kinases for potential anticancer drugs. *Bioorg Med Chem*. 2019;27:677–85.
14. Patel K, Kumar V, Rahman M, Verma A, Patel DK. New insights into the medicinal importance, physiological functions and bioanalytical aspects of an important bioactive compound of foods 'Hyperin': health benefits of the past, the present, the future. *Beni-Suef Univ J Basic Appl Sci*. 2018;7:31–42.
15. Singh D, Mendonsa R, Koli M, Subramanian M, Nayak SK. Antibacterial activity of resveratrol structural analogues: a mechanistic evaluation of the structure-activity relationship. *Toxicol Appl Pharmacol*. 2019;367:23–32.
16. De Filippis B, Ammazalorso A, Amoroso R, Giampietro L. Stilbene derivatives as new perspective in antifungal medicinal chemistry. *Drug Dev Res*. 2019;80:285–93.
17. Dvorakova M, Landa P. Anti-inflammatory activity of natural stilbenoids: a review. *Pharmacol Res*. 2017;124:126–45.
18. De Filippis B, Ammazalorso A, Fantacuzzi M, Giampietro L, Maccallini C, Amoroso R. Anticancer activity of stilbene-based derivatives. *ChemMedChem*. 2017;12:558–70.
19. Pecyna P, Wargula J, Murias M, Kucinska M. More than resveratrol: new insights into stilbene-based compounds. *Biomolecules*. 2020;10:1–40.
20. Wen L, Jiang Y, Yang J, Zhao Y, Tian M, Yang B. Structure, bioactivity, and synthesis of methylated flavonoids. *Ann NY Acad Sci*. 2017;1398:120–9.
21. Kluska M, Jabłońska J, Prukała W. Analytics, properties and applications of biologically active stilbene derivatives. *Molecules*. 2023;28(11):4482.
22. Moore DD, Kato S, Xie W, Mangelsdorf DJ, Schmidt DR, Xiao R, et al. International union of pharmacology. LXII. The NR1H and NR1I receptors: constitutive androstane receptor, pregnane X receptor, farnesoid X receptor alpha, farnesoid X receptor beta, liver X receptor alpha, liver X receptor beta, and vitamin D receptor. *Pharmacol Rev*. 2006;58:742–59.
23. Zhang W, Go ML. Quinone reductase induction activity of methoxylated analogues of resveratrol. *Eur J Med Chem*. 2007;42:841–50.
24. Chang S-L, Chiang Y-M, Chang CL-T, Yeh H-H, Shyur L-F, Kuo Y-H, et al. Flavonoids, centaurein and centaureidin, from *Bidens pilosa*, stimulate IFN-gamma expression. *J Ethnopharmacol*. 2007;112:232–6.
25. Lui ACW, Pow KC, Lin N, Lam LPY, Liu G, Godwin ID, et al. Regioselective stilbene O-methylations in *Saccharinae* grasses. *Nat Commun*. 2023;14:3462.
26. Kumar S, Pandey AK. Chemistry and biological activities of flavonoids: an overview. *Sci World J*. 2013;2013:1–16.
27. Cho MH, Park HL, Park JH, Lee SW, Bhoo SH, Hahn TR. Characterization of regiospecific flavonoid 3',5'-O-methyltransferase from tomato and its application in flavonoid biotransformation. *J Korean Soc Appl Biol Chem*. 2012;55:749–55.
28. Cui H, Song MC, Ban YH, Jun SY, Kwon AS, Lee JY, et al. High-yield production of multiple O-methylated phenylpropanoids by the engineered *Escherichia coli*-*Streptomyces* cocultivation system. *Microb Cell Fact*. 2019;18:1–13.
29. Yoon Y. Characterization of an O-methyltransferase from *Streptomyces avermitilis* MA-4680. *J Microbiol Biotechnol*. 2010;20:1359–66.
30. Yoon Y, Yi YS, Lee Y, Kim S, Kim BG, Ahn J-H, et al. Characterization of O-methyltransferase ScOMT1 cloned from *Streptomyces coelicolor* A3(2). *Biochim Biophys Acta Gene Struct Expr*. 2005;1730:85–95.
31. Darsandhari S, Dhakal D, Shrestha B, Parajuli P, Seo J-H, Kim T-S, et al. Characterization of regioselective flavonoid O-methyltransferase from the *Streptomyces* sp. KCTC 0041BP. *Enzyme Microb Technol*. 2018;113:29–36.
32. Parajuli P, Pandey RP, Nguyen THT, Dhakal D, Sohng JK. Substrate scope of O-methyltransferase from *Streptomyces peucetius* for biosynthesis of diverse natural products methoxides. *Appl Biochem Biotechnol*. 2018;184:1404–20.
33. Pérez-Valero Á, Serna-Diestro J, Tafur Rangel A, Barbuo Ferraiuolo S, Schiraldi C, Kerkhoven EJ, et al. Biosynthesis of hesperetin, homoeriodictyol, and homoheesperetin in a transcriptomics-driven engineered strain of *Streptomyces albidoflavus*. *Int J Mol Sci*. 2024;25:4053.
34. Pérez-Valero Á, Serna-Diestro J, Villar CJ, Lombó F. Use of 3-deoxy-D-arabino-heptulosonic acid 7-phosphate synthase (DAHP synthase) to enhance the heterologous biosynthesis of diosmetin and chrysoeriol in an engineered strain of *Streptomyces albidoflavus*. *Int J Mol Sci*. 2024;25:2776.
35. Farkašová J, Godány A, Vlček Č. Identification of a holin encoded by the *Streptomyces aureofaciens* phage μ 1/6; functional analysis in *Escherichia coli* system. *Folia Microbiol*. 2004;49:679–84.
36. Myronovskiy M, Luzhetskyy A. Native and engineered promoters in natural product discovery. *Nat Prod Rep*. 2016;33:1006–19.
37. Kim B-G, Jung B-R, Lee Y, Hur H-G, Lim Y, Ahn J-H. Regiospecific flavonoid 7-O-methylation with *Streptomyces avermitilis* O-methyltransferase expressed in *Escherichia coli*. *J Agric Food Chem*. 2006;54:823–8.
38. Yokotsuka K, Okuda T. Light-induced isomerization of trans-resveratrol to cis-resveratrol in must and wine during fermentation and storage. *J ASEV Jpn*. 2011;22:16–21.
39. Figueiras TS, Neves-Petersen MT, Petersen SB. Activation energy of light induced isomerization of resveratrol. *J Fluoresc*. 2011;21:1897–906.
40. Hui Y, Li X, Chen X. Assessment for the light-induced cis-trans isomerization of rhapontigenin and its glucoside rhaponticin by capillary electrophoresis and spectrometric methods. *J Chromatogr A*. 2011;1218:5858–66.
41. Reuhs BL. Production of cell-associated polysaccharides of *Rhizobium fredii* USDA205 is modulated by apigenin and host root extract. *Mol Plant-Microbe Interact*. 1994;7:240.
42. Schubert HL, Blumenthal RM, Cheng X. Many paths to methyltransfer: a chronicle of convergence. *Trends Biochem Sci*. 2003;28:329–35.
43. Choi K, Jung E, Yang Y, Kim B. Production of a novel O-methyl-isoflavone by regioselective sequential hydroxylation and O-methylation reactions in *Streptomyces avermitilis* host system. *Biotechnol Bioeng*. 2013;110:2591–9.
44. Koirala N, Pandey RP, Parajuli P, Jung HJ, Sohng JK. Methylation and subsequent glycosylation of 7,8-dihydroxyflavone. *J Biotechnol*. 2014;184:128–37.
45. Dhar K, Rosazza JPN. Purification and characterization of *Streptomyces griseus* catechol O-methyltransferase. *Appl Environ Microbiol*. 2000;66:4877–82.
46. Malla S, Koffas MAG, Kazlauskas RJ, Kim B-G. Production of 7-O-methyl aromadendrin, a medicinally valuable flavonoid, in *Escherichia coli*. *Appl Environ Microbiol*. 2012;78:684–94.
47. Zhang Y, Han M-Z, Zhu S-L, Li M, Dong X, Luo X-C, et al. Studies on the function and catalytic mechanism of O-methyltransferases SviOMT02, SviOMT03 and SviOMT06 from *Streptomyces virginiae* IBL14. *Enzyme Microb Technol*. 2015;73–74:72–9.
48. Jansson A, Koskiniemi H, Mäntsälä P, Niemi J, Schneider G. Crystal structure of a ternary complex of DnrK, a methyltransferase in daunorubicin biosynthesis, with bound products. *J Biol Chem*. 2004;279:41149–56.
49. Shin W, Lah MS. Structure of (R, S)-naringenin. *Acta Crystallogr Sect C Cryst Struct Commun*. 1986;42:626–8.
50. Aisa HA, Izotova L, Karimov A, Botirov E, Mamadrahimov A, Ibragimov B. Crystal, molecular structure and hirshheld surface analysis of 5-hydroxy-3,6,7,8-tetramethoxyflavone. *Acta Crystallogr Sect E Crystallogr Commun*. 2020;76:1748–51.
51. Cuyckens F, Claeys M. Mass spectrometry in the structural analysis of flavonoids. *J Mass Spectrom*. 2004;39:1–15.
52. Li C, Schmidt A, Pichersky E, Shi F, Jones AD. Identification of methylated flavonoid regioisomeric metabolites using enzymatic semisynthesis and liquid chromatography-tandem mass spectrometry. *Metabolomics*. 2013;9:92–101.

53. Nishimura M, Nishimura Y, Abe C, Kohhata M. Expression and substrate range of *Streptomyces* vanillate demethylase. *Biol Pharm Bull.* 2014;37:1564–8.
54. Jourdan S, Francis IM, Deflandre B, Tenconi E, Riley J, Planckaert S, et al. Contribution of the β -glucosidase BglC to the onset of the pathogenic lifestyle of *Streptomyces scabies*. *Mol Plant Pathol.* 2018;19:1480–90.
55. Gu M-Z, Wang J-C, Liu W-B, Zhou Y, Ye B-C. Expression and displaying of β -glucosidase from *Streptomyces coelicolor* A3 in *Escherichia coli*. *Appl Biochem Biotechnol.* 2013;170:1713–23.
56. Moldoveanu N, Kluepfel D. Comparison of β -glucosidase activities in different *Streptomyces* strains. *Appl Environ Microbiol.* 1983;46:17–21.
57. Jędrzejewski M, Szeleszczuk Ł, Pisklak DM. The reaction mechanism of loganic acid methyltransferase: a molecular dynamics simulation and quantum mechanics study. *Molecules.* 2023;28:5767.
58. MacNeil DJ, Gewain KM, Ruby CL, Dezeny G, Gibbons PH, MacNeil T. Analysis of *Streptomyces avermitilis* genes required for avermectin biosynthesis utilizing a novel integration vector. *Gene.* 1992;111:61–8.
59. Matera A, Dulak K, Sordon S, Waśniewski K, Huszcza E, Popłoński J. Evaluation of double expression system for co-expression and co-immobilization of flavonoid glucosylation cascade. *Appl Microbiol Biotechnol.* 2022;106:7763–78.
60. Chater KF, Wilde LC. *Streptomyces albus* G mutants defective in the SalGI restriction–modification system. *J Gen Microbiol.* 1980;116:323–34.
61. Kieser T, Bibb MJ, Buttner MJ, Chater KF, Hopwood DA, et al. *Practical Streptomyces genetics*. Norwich: John Innes Foundation Norwich; 2000.
62. Taylor T, Denson J-P, Esposito D. Optimizing expression and solubility of proteins in *E. coli* using modified media and induction parameters. *Methods Mol Biol.* 2017;1586:65–82. https://doi.org/10.1007/978-1-4939-6887-9_5.
63. Dulak K, Sordon S, Matera A, Kozak B, Huszcza E, Popłoński J. Novel flavonoid C-8 hydroxylase from *Rhodotorula glutinis*: identification, characterization and substrate scope. *Microb Cell Fact.* 2022;21:175.
64. Bradford MM. A rapid and sensitive method for the quantitation of microgram quantities of protein utilizing the principle of protein–dye binding. *Anal Biochem.* 1976;72:248–54.
65. Magadán-Corpas P, Ye S, Pérez-Valero Á, McAlpine PL, Valdés-Chiara P, Torres-Bacete J, et al. Optimized de novo eriodictyol biosynthesis in *Streptomyces albidoflavus* using an expansion of the golden standard toolkit for its use in actinomycetes. *Int J Mol Sci.* 2023;24(10):8879.
66. García-Gutiérrez C, Aparicio T, Torres-Sánchez L, Martínez-García E, de Lorenzo V, Villar CJ, et al. Multifunctional SEVA shuttle vectors for actinomycetes and Gram-negative bacteria. *MicrobiologyOpen.* 2020;9:1135–49.
67. Blázquez B, Torres-Bacete J, Leon DS, Kniewel R, Martínez I, Sordon S, et al. Golden standard: a complete standard, portable, and interoperative MoClo tool for model and non-model bacterial hosts. *bioRxiv.* 2022. <https://doi.org/10.1101/2022.09.20.508659>.

Publisher's Note

Springer Nature remains neutral with regard to jurisdictional claims in published maps and institutional affiliations.